



Cite this: *Energy Environ. Sci.*, 2020, 13, 4204

## What is needed to deliver carbon-neutral heat using hydrogen and CCS?†

Nixon Sunny, <sup>ab</sup> Niall Mac Dowell <sup>\*ac</sup> and Nilay Shah<sup>\*ab</sup>

In comparison with the power sector, large scale decarbonisation of heat has received relatively little attention at the infrastructural scale despite its importance in the global CO<sub>2</sub> emissions landscape. In this study we focus on the regional transition of a heating sector from natural gas-based infrastructure to H<sub>2</sub> using mathematical optimisation. A discrete spatio-temporal description of the geographical region of Great Britain was used in addition to a detailed description of all network elements for illustrating the key factors in the design of nation-wide H<sub>2</sub> and CO<sub>2</sub> infrastructure. We have found that the synergistic deployment of H<sub>2</sub> production technologies such as autothermal reforming of methane, and biomass gasification with CO<sub>2</sub> abatement technologies such as carbon capture and storage (CCS) are critical in achieving cost-effective decarbonisation. We show that both large scale underground H<sub>2</sub> storage and water electrolysis provide resilience and flexibility to the heating system, competing on cost and deployment rates. The optimal regions for siting H<sub>2</sub> production infrastructure are characterised by proximity to: (1) underground H<sub>2</sub> storage, (2) high demands for H<sub>2</sub>, (3) geological storage for CO<sub>2</sub>. Furthermore, cost-effective transitions based on a methane reforming pathway may necessitate regional expansions in the supply of natural gas with profound implications for security of supply in nations that are already highly reliant, potentially creating an infrastructure lock-in during the near term. We found that the total system cost, comprising both investment and operational elements, is mostly influenced by the natural gas price, followed by biomass price and CapEx of underground caverns. Under a hybrid Regulated Asset Base (RAB) commercial framework, with private enterprises delivering production infrastructure, the total cost of heat supply over the infrastructure lifetime is estimated as 5.2–8.6 pence per kW h. Due to the higher cost relative to natural gas, a Contract for Difference payment between £20 per MW h and £53 per MW h will be necessary for H<sub>2</sub>-derived heat to be competitive in the market.

Received 24th June 2020,  
Accepted 22nd September 2020

DOI: 10.1039/d0ee02016h

rsc.li/ees



### Broader context

Decarbonising the heating sector in the global economy presents infrastructural and social challenges, especially for those nations that are reliant on natural gas for heat provision. Fuel poverty is a major issue that affects a significant portion of people in the developed world, with the lack of affordable heat being a key determinant of excess winter deaths. It is imperative that access to affordable heat is increased during the transition towards net-zero greenhouse gas emissions. In this context, there is growing evidence to indicate that the co-deployment of H<sub>2</sub> and CO<sub>2</sub> infrastructure may facilitate a sustainable energy transition from the incumbent natural gas infrastructure to a carbon-neutral future. Yet, there is little understanding of the requirements of the transition (*i.e.*, investment locations, extent of financial support, and rates of deployment) to support this ambition. Moreover, the impact of geographical considerations related to resource and storage availability on the economic feasibility of technology investments are poorly understood. In this study, we present a systematic assessment of the regional conversion of the natural gas supply chain to H<sub>2</sub>, accounting for all the processing elements within both H<sub>2</sub> and CO<sub>2</sub>-integrated value chains. We compare the overall primary energy consumption of the designed system relative to the incumbent infrastructure to identify regional implications for resource use. Key questions that are addressed in this work include: (a) what is the required scale of technology deployment?, (b) what are the regional factors that determine optimal investment locations?, (c) what is the cost of heat supply using H<sub>2</sub> and what is necessary for it to be affordable?

<sup>a</sup> Centre for Process Systems Engineering, Imperial College London, Exhibition Road, London, SW7 2AZ, UK. E-mail: niall@imperial.ac.uk, n.shah@imperial.ac.uk

<sup>b</sup> Department of Chemical Engineering, Imperial College London, Exhibition Road, London, SW7 2AZ, UK

<sup>c</sup> Centre for Environmental Policy, Imperial College London, Exhibition Road, London, SW7 1NA, UK

† Electronic supplementary information (ESI) available. See DOI: 10.1039/d0ee02016h

## 1 Introduction

### 1.1 Challenges and knowledge gaps

A growing need for climate change mitigation has led to the establishment of ambitious legislation by advanced economies, such as the United Kingdom (UK), France, and Norway to an

economy-wide transition to net-zero greenhouse gas emissions by 2050.<sup>1</sup> In this context, progress in the decarbonisation of the heating sector has lagged significantly behind the electricity sector<sup>2</sup> and requires concerted attention. Heating and cooling related consumption accounts for half of the primary energy consumption in the European Union (EU).<sup>3</sup> At present, natural gas is used to supply nearly half of the EU heat demand with national shares as high as 80% in the Netherlands and the UK.<sup>4,5</sup> Growing energy demands, coupled with unique geological conditions (access to low-cost gas production and underground storage), are likely to have cemented the establishment of natural gas networks in such regions.<sup>6–10</sup> In this context, a H<sub>2</sub>-based heating supply may provide an attractive opportunity for “low-carbon” infrastructural transitions in these regions due to its ability to reutilise the existing gas infrastructure whilst providing consumers with affordable heat using familiar technologies.

There is an ongoing debate on the optimal set of technologies for the deployment of “low-carbon” H<sub>2</sub> in order to supply the near term demand. Globally, methane and coal-based technologies currently dominate the dedicated H<sub>2</sub> production capacity (approximately 70 Mt year<sup>-1</sup>) with shares of 76% (used in Middle East, EU, Russia, United States, *etc.*) and 23% (mainly used within the People's Republic of China) respectively.<sup>15</sup> The remaining 1% is produced *via* water electrolysis (WE). There is great uncertainty as to the value offered by alternative production technologies for the generation of H<sub>2</sub> in a CO<sub>2</sub>-neutral environment. As discussed in Appendix A.2, there are a wide variety of commercially available technology options for the production of H<sub>2</sub>. Fig. 1 illustrates that at the time of writing, heating pathways relying on H<sub>2</sub> from existing fuels without carbon capture and storage (CCS) are untenable in the long-term as they are more CO<sub>2</sub>-intensive than the direct combustion of natural gas. The future deployment potential of WE at scale will be dependent on achieving net-zero CO<sub>2</sub> emissions from the power sector. Importantly, WE has a lower CO<sub>2</sub> footprint compared to autothermal reforming (ATR) with CCS only when the CO<sub>2</sub> intensity of the power supply is less than 10 g kW<sup>-1</sup>. Negative emissions technologies (NETs) such as biomass gasification or biomass combined heat & power (CHP) with CCS may have an important role due to their unique ability to supply heat whilst removing CO<sub>2</sub> from the atmosphere. Overall, the deployment potential of any technology is likely to be influenced by its CO<sub>2</sub> intensity, feedstock prices and its availability. Hence, they must be incorporated in planning to identify the most relevant technology choices in a CO<sub>2</sub>-neutral environment.

## 1.2 Existing literature

One of the earliest attempts at devising a robust mathematical model of a H<sub>2</sub> supply chain (HSC) network was achieved by Van Den Heever and Grossmann in 2003.<sup>16</sup> Their work considered a set of pre-defined nodes representing production facilities with inter-connecting pipelines and customers, with emphasis on the planning and scheduling of the network. However, this methodology failed to account for the deployment of new infrastructure. This gap was addressed in 2006, when Almansoori and Shah presented general frameworks for HSC

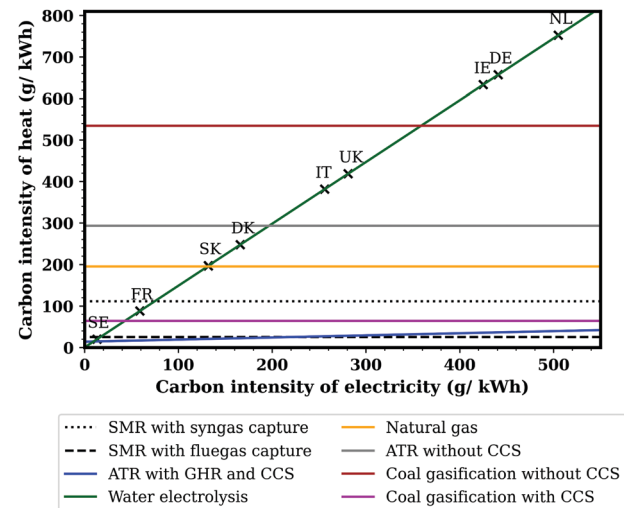


Fig. 1 CO<sub>2</sub> intensity of heat provision for various technologies, excluding the generation of greenhouse gas emissions during material extraction, construction, transportation, and decommissioning. A boiler conversion efficiency of 94%<sup>11</sup> and a natural gas CO<sub>2</sub> intensity of 184 g kW h<sup>-1</sup> (ref. 12) are assumed for the feedstock. Due to the fact that ATRs with gas heating reforming (GHR) and CCS are net importers of power, their overall CO<sub>2</sub> intensity has a weak dependency on the electricity grid. Coal gasification assumes a bituminous coal feed with an energy content of 8.4 kWh kg<sub>HHV</sub><sup>-1</sup> and an achievable CO<sub>2</sub> capture rate of 88% when relevant.<sup>13</sup> Markers represent the CO<sub>2</sub> intensity of heat achievable through WE if the indicated nations use their electricity grid as the power supply, based on 2016 estimates from the European Environment Agency.<sup>14</sup> Country names are as follows: Sweden (SE), France (FR), Slovakia (SK), Denmark (DK), Italy (IT), United Kingdom (UK), Ireland (IE), Germany (DE), Netherlands (NL).

design and operation.<sup>17–19</sup> A large number of studies have further explored the design of HSCs in various geographical contexts for an extensive array of applications.<sup>20–34</sup>

To the best of the authors' knowledge, Moreno-Benito *et al.*<sup>33</sup> is the only study that has considered spatially-explicit, simultaneous development of both H<sub>2</sub> and CO<sub>2</sub> value chains to support the decarbonisation of the transportation system. Similarly, little attention has been paid to the development of HSCs for the decarbonisation of heat as an energy vector with only a single publication by Samsatli and Samsatli to the authors' knowledge.<sup>35</sup> They studied the role of renewable H<sub>2</sub> and electrification in decarbonising heat and found that complete electrification is preferable in the absence of large scale H<sub>2</sub> storage. However, the potential for H<sub>2</sub> to replace the existing heat demand from natural gas and achieve CO<sub>2</sub>-neutrality needs further investigation. Furthermore, the role of methane-based technologies with CCS and NETs remain critically unexplored.

Moreno-Benito *et al.*<sup>33</sup> conclude that steam methane reforming (SMR) with CCS is the most economical production technology as CO<sub>2</sub> emissions are minimised. However, the benefits of advanced reforming technologies to a CO<sub>2</sub>-neutral environment is unclear. They also indicate the importance of WE as a low-carbon generation technology, which is unlikely to be relevant for net-zero CO<sub>2</sub> emissions without drastic reductions in the electricity grid CO<sub>2</sub> intensity towards CO<sub>2</sub>-neutrality. Furthermore, the effect of natural gas grid CO<sub>2</sub> intensity and the availability of negative

emissions on the optimal technology selection, and total costs associated with decarbonisation, remains an open question.

A substantial proportion of research addressing the design of HSCs has focused on H<sub>2</sub> as the sole energy vector capable of supplying consumer demands (*i.e.*, H<sub>2</sub> for supplying transportation demands). This is evidenced in publications such as Johnson *et al.*,<sup>36</sup> De-Leon Almaraz *et al.*,<sup>37</sup> Nunes *et al.*<sup>31</sup> amongst many others. It must be noted that earlier attempts at modelling HSCs were aimed at analysing the design of HSCs rather than define its role in a diverse energy mix. Such approaches are often restrictive in their ability to consider transitions from incumbent infrastructure as there are no descriptions of existing fuels and infrastructure.

In general, infrastructures are spatially constituted and therefore, influenced by regional factors. At the time of writing, to the best of the authors' knowledge, no studies have sought to model a spatially explicit transition from the incumbent infrastructure to a decarbonised future for the heating sector. The development of structured decarbonisation trajectories, which incorporate strategic regional opportunities, can reduce the cost of heat infrastructure. Thus, optimal regions for low-carbon investment must be identified to aid gas-reliant nations to plan for a decarbonised future.

### 1.3 Contributions from this study

This contribution provides economic and environmental assessments of the conversion of a natural gas-based heating supply system to H<sub>2</sub>. To this end, a mathematical programming approach was utilised to study the long-term potential for H<sub>2</sub> and CCS technologies using the geographical region of Great Britain (GB) as an instantiated case study. The authors intend to provide a comprehensive view of a H<sub>2</sub>-based heating system as a structured basis for comparison with alternative future visions on decarbonisation of heat. In addition, this study decomposes the design complexities and identifies a set of reducible engineering considerations that favour the use of a H<sub>2</sub> network within a geographical context for broader relevance. In particular, the robustness of H<sub>2</sub>-based solutions and their dependencies on existing natural gas/electricity grid infrastructure, resource prices and NETs are studied.

The mixed integer linear programming (MILP) framework presented in this paper is based on the Resource Technology Network (RTN) framework and combines all components of both H<sub>2</sub> and CO<sub>2</sub> value chains into a single decision-making framework, where the optimal choices of production, transportation and storage technologies are determined on a regional basis to support the transition into a low-carbon H<sub>2</sub> network. The mathematical model contains explicit definitions of primary resources such as natural gas, electricity and biomass. This is accompanied with a description of production technologies such as biomass gasification and methane reforming with CCS along with the water electrolysis process. Geological storage of H<sub>2</sub> in underground caverns and CO<sub>2</sub> in offshore basins are described. The heating demand segment in this study includes domestic and non-domestic users that are connected to the existing gas network.

The remainder of this paper is structured as follows. Section 2 describes the spatio-temporal characteristics of heat demand, and the key methodological relations between model variables are summarised in Section 3. Section 4 presents the role of different technologies in achieving cost-effective CO<sub>2</sub> mitigation and their implications for storage and resource use. Section 5 details infrastructure deployment analyses and identifies regional dependencies that greatly influence the nature of the transition into a H<sub>2</sub> supply. Section 6 evaluates the total cost of the various infrastructure components and exposes key factors that determine the economic viability of the designed system. Section 7 synthesises the findings from the earlier sections for relevance to regions that rely on gas-based heating.

## 2 Spatio-temporal description of demand

### 2.1 Demand modelling

In general, the demand for heating can be decomposed into two components: (a) a domestic heating component, which is characterised by significant temporal variation, and; (b) a non-domestic heating<sup>‡</sup> component which is assumed to be time invariant across the annual time horizon. The input data used to describe the spatial distribution of heating demand was obtained from the Department for Business, Energy & Industrial Strategy (BEIS)<sup>38</sup> within Her Majesty's Government (HMG); it presents meter records of natural gas consumption for domestic and non-domestic users in GB. Approximately 38 TW h (7%) of natural gas consumption was not attributable to any location due to reasons such as insufficient meter readings, non-disclosure of consumption data, *etc.* Natural gas is assumed to be used wholly for heating purposes within the domestic context. In contrast, non-domestic natural gas consumption is not limited to heating as some users may use natural gas as feedstock. However, the reported data is used to generate the total non-domestic heating demand, as a conservative estimate. The authors note that this data does not represent total GB heating demands as approximately 15% of buildings are not connected to the gas network and use alternative forms of heating.

Rosenow *et al.*<sup>39</sup> estimates a cost-effective, energy efficiency improvement of 18% in existing buildings in the UK by 2035, without the inclusion of technologies such as heat pumps or heat networks. The UK population is expected to increase from 66 million to 77 million by 2050 according to the Office for National Statistics.<sup>40</sup> Assuming a proportional increase in heating consumption with population growth, a 17% increase in total demand may be apparent by 2050. Overall, the total heat consumption is assumed constant at present values over each year in the planning horizon mainly due to long-term projection uncertainties and since the aforementioned effects balance each other.

<sup>‡</sup> Non-domestic use refers to commercial buildings and small industrial sites.



## 2.2 Regional clusters

Fig. 2 illustrates the spatial variations in GB's annual natural gas consumption for both domestic and non-domestic heat provision. Of the total, 63% is consumed by the domestic sector, with the balance accounted for by the non-domestic sector. This data is further categorised into heating demand density bands in Table 1. Almost 70% of the nation's total heating related consumption arises from only 7% of its total area. A distinctive feature of the heating system is that regional demand is clustered in line with population density and industrial activity. This means that decarbonising the top 5 regional clusters would mitigate 60% of total nation-wide heat emissions.

## 2.3 Temporal variability

The temporal variation in the domestic heating demand profile over an annual time horizon is described in Fig. 3. This dataset was obtained from Sansom.<sup>41</sup> These time-based variations were scaled appropriately to merge with the spatial consumption data to form annual consumption estimates. Sansom estimates the load factor of heat demand in GB to be almost a quarter of that of the electricity demand<sup>41</sup> (*i.e.*, a four-fold increase in variability relative to electricity). This highlights the need for infrastructure that is highly responsive to load variations.

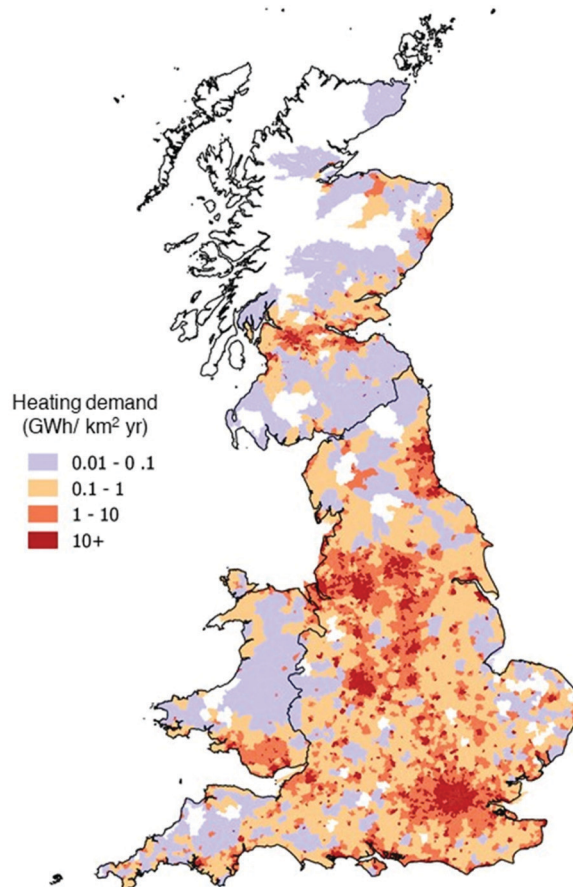


Fig. 2 Spatial distribution of heating demand densities in the geographical region of Great Britain.

Table 1 Domestic and non-domestic heating demand densities and area band statistics for Great Britain

Heating demand density (GW h km <sup>-2</sup> year <sup>-1</sup> )	Area (km <sup>2</sup> )	Share of the total area (%)	Total demand (GW h)	Share of the total heat demand (%)
0–0.1	61 800	33	1 900	0.5
0.1–1	76 100	41	29 300	6.5
1–10	35 400	19	110 000	24
10+	12 600	7	315 000	69

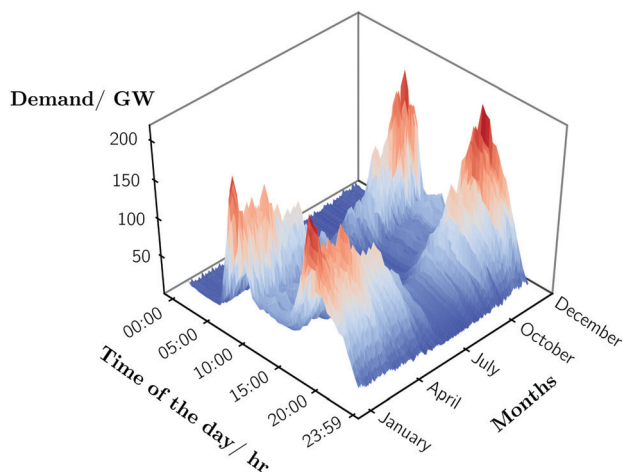


Fig. 3 Temporal distribution of domestic heating demand over an annual time horizon.

## 3 Methodology

The RTN modelling framework, used in this study, was originally developed by Pantelides.<sup>57</sup> Key characteristics of this decision-making framework are its ability to explicitly model spatio-temporal variations in addition to resources and technologies. This framework has been extensively used by a number of investigators, including Zhang and Sargent,<sup>58</sup> Schilling and Pantelides,<sup>59,60</sup> Dimitriaidis *et al.*,<sup>61</sup> Castro *et al.*,<sup>62–64</sup> and recently by Samsatli *et al.*<sup>65</sup>

A detailed summary of the technologies for H<sub>2</sub> and CO<sub>2</sub> value chains are presented in Appendix A. Further methodological innovations are described in detail in Section S2 of the ESI.† A diagrammatic representation of the analytical superstructure is depicted in Fig. 4. The key technology options within the model formulation are summarised in Tables 2–4. End-use technologies are not analysed as the study is framed to evaluate the conversion of the natural gas supply to H<sub>2</sub>. Dorrington *et al.*<sup>66</sup> has indicated that boiler manufacturers have the capacity to scale up the production of H<sub>2</sub>-fired appliances in line with the UK heating appliance demand. Furthermore, the cost of domestic H<sub>2</sub> boilers are assumed to be comparable to natural gas boilers, at the production scales that are required by this study.<sup>11</sup> Additionally, Dodds *et al.*<sup>67</sup> discusses the various developments in fuel cell technology for the provision of heat. As such, consumers are likely to purchase end-use appliances depending on their preferences and needs.



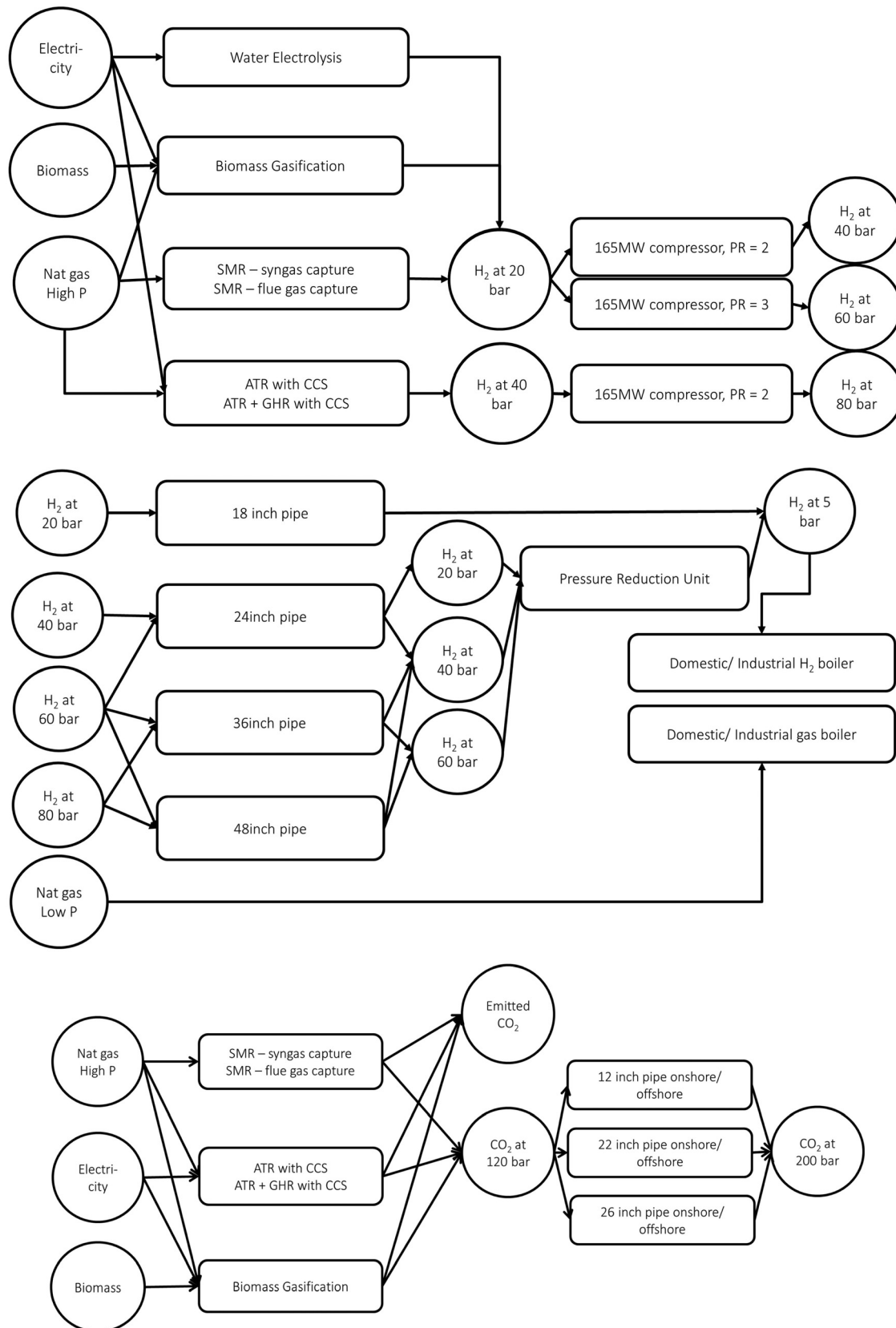


Fig. 4 The analytical superstructure of the optimisation model with resource states indicated as circles and technologies as rectangles with rounded corners. The image summarises important model components with the exception of storage technologies.



**Table 2** H<sub>2</sub> production technologies and their techno-economic characteristics are summarised here. Conventional SMR plants may be integrated with CO<sub>2</sub> capture from the shifted syngas, using chemical solvents to achieve an overall reduction of 55% of emissions. Alternatively, an amine-based capture unit can be integrated with the outlet flue gas of the reformer to achieve an approximate CO<sub>2</sub> reduction of 90%. In autothermal reforming with CCS, the heat for the reforming reaction is supplied by partial combustion of the reformer feed with O<sub>2</sub>, allowing greater quantities of CO<sub>2</sub> to be captured economically. Gas heating reforming (GHR) can be integrated with ATRs and CCS to recover some of the heat generated at high pressures and temperatures in order to reduce the O<sub>2</sub> and feed consumption, hence achieve higher efficiencies. Natural gas is assumed to have a CO<sub>2</sub> intensity of 184 g kW h<sup>-1</sup> (ref. 12) and the CO<sub>2</sub> intensity of H<sub>2</sub> production does not report supply chain emissions. Appendix A.2 contains a detailed description of the production technologies, their techno-economic assumptions alongside their operating characteristics. Note that HHV in the table below refers to the higher heating value of H<sub>2</sub>

Technology type	Plant size (MW HHV)	CapEx (£ per kW)	Efficiency (% HHV)	CO <sub>2</sub> intensity (g per kW per h)
SMR with syngas capture <sup>42–44</sup>	1000	320	73	105
SMR with fluegas capture <sup>11,42,43</sup>	1000	480	70	23.8
ATR with CCS <sup>11,13</sup>	1000	510	78	15
ATR with GHR and CCS <sup>11,13</sup>	1000	490	83	13
Water electrolysis <sup>15,45,46</sup>	100	880	72	1.4 × CI <sub>electricity</sub>
Biomass gasification with CCS <sup>11,47–49</sup>	200	1100	40	−420

**Table 3** Pipelines of various sizes are considered as a means of transportation of both H<sub>2</sub> and CO<sub>2</sub>. Maximum flowrates of each resource through the pipelines were evaluated using the pipeline specifications, in addition to approximate environment conditions, assuming a maximum pressure drop of 20 barg for H<sub>2</sub> over 80–100 km distance. Similarly, maximum CO<sub>2</sub> flowrates were computed on the basis of the pressure ranges in order to maintain the resource in dense phase during transportation. Further details on the analytical procedure can be found in Appendix A.1

Technology type	Maximum flow rate (kg s <sup>-1</sup> )	CapEx (£k per km)	Assumed losses (%/km)
H <sub>2</sub> pipeline – 18 inch	7.1	870 <sup>11</sup>	0.005 <sup>50</sup>
H <sub>2</sub> pipeline – 24 inch	30	1260 <sup>11</sup>	0.005 <sup>50</sup>
H <sub>2</sub> pipeline – 36 inch	105	2020 <sup>11</sup>	0.005 <sup>50</sup>
H <sub>2</sub> pipeline – 48 inch	220	2790 <sup>11</sup>	0.005 <sup>50</sup>
Onshore CO <sub>2</sub> pipeline – 12 inch	88	600 <sup>11</sup>	0.002 <sup>51</sup>
Onshore CO <sub>2</sub> pipeline – 26 inch	350	1300 <sup>11</sup>	0.002 <sup>51</sup>
Offshore CO <sub>2</sub> pipeline – 12 inch	88	780 <sup>11</sup>	0.002 <sup>51</sup>
Offshore CO <sub>2</sub> pipeline – 26 inch	350	1500 <sup>11</sup>	0.002 <sup>51</sup>

### 3.1 Key model constraints

**3.1.1 Resource balance.** Eqn (1) is a key relation in the model, encompassing the operational elements of all the model components as discussed in prior sections. The equation below includes  $\varepsilon_{r,g,t,tm}$ , which is an emission rate term necessary to

**Table 4** Storage technologies for H<sub>2</sub> and CO<sub>2</sub> and their performance characteristics are summarised here. Approximate injectivity and deliverability rates for H<sub>2</sub> are reported from literature.<sup>13,52</sup> The CapEx per storage cavern was calculated assuming an average CapEx of £500 per MW h H<sub>2</sub> as a conservative estimate.<sup>13,53,54</sup> Further information on storage capacity can be found in Appendix A.4. In contrast, storing natural gas in caverns can achieve storage capacities of 230 GW h in medium pressure caverns and 500 GW h in high pressure caverns based on the data from National Institute of Standards and Technology<sup>55</sup>

Technology type	Capacity (GW h)	Maximum injectivity	Maximum deliverability (GW h)	CapEx (£m per unit)
Medium pressure cavern <sup>13,53</sup>	64	100 MW <sup>13</sup>	200 MW <sup>13</sup>	32
High pressure cavern <sup>13,53</sup>	144	100 MW <sup>13</sup>	200 MW <sup>13</sup>	100
CO <sub>2</sub> injection well	—	1.5 Mt year <sup>−1</sup> <sup>56</sup>	—	66 <sup>56</sup>

this model instance. The equation is described as follows:

$$\text{IM}_{r,g,t,tm} - D_{r,g,t,tm} - \varepsilon_{r,g,t,tm} + \sum_{pj} \mu_{pj,r} P_{pj,g,t,tm} + \sum_{d,g',dmo} \beta_{r,dm,d} Q_{g',g,d,dmo,t,tm} + \sum_{sj} \lambda_{r,g,sj,t,tm}^S - \sum_{d,g',dmo} \beta_{r,dm,d} Q_{g,g',d,dmo,t,tm} - \sum_{sj} \lambda_{r,g,sj,t,tm}^R = 0 \quad \forall r, g, t, tm \quad (1)$$

where IM<sub>r,g,t,tm</sub> denotes the import rate of a resource *r* in cell *g* at minor time *t* and major time *tm*, D<sub>r,g,t,tm</sub> is the demand of a resource, P<sub>pj,g,t,tm</sub> denotes the production rate of a resource through process technology, *pj*. Q<sub>g',g,d,dmo,t,tm</sub> describes the inlet flowrate of a resource through a distribution technology *d* and distribution mode, *dmo*, whereas Q<sub>g,g',d,dmo,t,tm</sub> describes the outflow from a region, λ<sub>r,g,sj,t,tm</sub><sup>S</sup> is the storage rate of a resource using storage technology *sj* and λ<sub>r,g,sj,t,tm</sub><sup>R</sup> is the retrieval rate. This is a universal relation for all resources in all regions at all time periods.

**3.1.2 Capacity constraints.** Eqn (2) introduces the capacity constraint on the production rate of a process technology. Similar equations are written for distribution and storage technologies.

$$P_{pj,g,t,tm} \leq N_{pj,g,tm}^P \text{NPC}_{pj} \quad \forall pj, g, t, tm \quad (2)$$

where N<sub>pj,g,tm</sub><sup>P</sup> is the number of process units of technology type *pj* in cell *g* at minor time *t* and major time *tm*, NPC<sub>pj</sub> is the nameplate capacity of the technology type *pj*. This equation applies to all process technologies that consume or produce resources and places a bound on the maximum production rate. In contrast, an equivalent form of the capacity constraint introduces a summation in the flow term across all distribution modes *dmo* when presented for the distribution technologies.

**3.1.3 Investment decisions.** The investment decisions are taken at every major time *tm* and influence the total number of available technologies at every point in the time horizon. Eqn (3) denotes the investment balance for process technologies.

$$N_{pj,g,tm}^P = N_{pj,g,tm-1}^P + NI_{pj,g,tm}^P \quad \forall pj, g, tm \quad (3)$$



where  $NI_{pj,g,tm}^P$  describes the additional number of process units installed in time period  $tm$ . This relation is applied to both the storage and distribution technologies.

**3.1.4 Performance metrics.** Eqn (4) computes the total value of each performance metric,  $m$  at major time,  $tm$ . The general form of the equation is presented here where the effects due to model components on the value of the performance metrics are evaluated. In this model formulation,  $m$  contains both CapEx and OpEx as set elements.

$$\begin{aligned} TM_{m,tm} = & \sum_{pj,g} \tau_{pj,g,m} NI_{pj,g,tm}^P + \sum_{r,sj,g} \tau_{sj,m} NI_{r,sj,g,tm}^S \\ & + \sum_{g,g',d} NC_{d,m} \nu_{g,g'} NI_{g,g',d,tm}^D + \sum_{pj,g,t} PC_{pj,m} P_{pj,g,t,tm} OT_t \\ & + \sum_{g,g',d,dmo,t} Q_{g,g',d,dmo,t,tm} QC_{d,m} OT_t \\ & + \sum_{ir,g,t} IMC_{ir,m} IM_{ir,g,t,tm} OT_t \\ & + \sum_{r,sj,g,t} SC_{sj,m} I_{r,g,sj,t,tm} \quad \forall m, tm \end{aligned} \quad (4)$$

where  $TM_{m,tm}$  is the total value of performance metrics at each  $tm$ ,  $\tau_{pj,g,m}$  is the effect on the performance metric from the investment of a process technology,  $\tau_{sj,m}$  is the effect on the performance metric from the investment of a storage technology,  $NC_{d,m}$  is the effect of the installation of a network using distribution technology  $d$ ,  $PC_{pj,m}$  is the effect due to consumption of resources using production technology,  $QC_{d,m}$  is the effect of flow of a resource through distribution technology  $d$ ,  $IMC_{ir,m}$  is the effect of importing resource,  $SC_{sj,m}$  is the effect of storing a resource using a storage technology,  $OT_t$  is the number of hours within each of the time periods,  $t$ . Additional terms are present in the equation within the modelling environment and they relate to the fixed effects arising from operation of the facilities over the time horizon adding to the OpEx. They have been omitted here for brevity.

**3.1.5 Emissions intensity.** Eqn (5) is used to denote the target reduction in overall  $\text{CO}_2$  emissions intensity. It incorporates a description of emissions intensities from the electricity grid, upstream methane supply chain and biomass supply in addition to the residual emissions arising from the operation of the  $\text{CO}_2$  capture facility. Negative emissions potential is attributed to biomass based technologies, where the  $\text{CO}_2$  removed using biomass results in negative  $\text{CO}_2$  release, counteracting the increases in emissions due to the usage of carbon intensive fuels. The equation is described as follows:

$$\sum_{g,t,tm} \frac{\left( \varepsilon_{a,g,t,tm} + \sum_r UE_r IM_{r,g,t,tm} - P_{b,g,t,tm} \mu_{b,a} \right) OT_t}{DEM^{\text{tot}}} CI \quad (5)$$

$a = \text{CO}_2$ ,  $b = \text{Biomass gasification with CCS}$

where the numerator represents the net emissions from the network and  $DEM^{\text{tot}}$  denotes the total demand for both

domestic and non-domestic heat in the network and  $CI$  represents an assigned parameter constraining the  $\text{CO}_2$  intensity of the designed network. In this study, a linear emission reduction trajectory is assumed, enabling path analysis from approximately  $200 \text{ g kWh}^{-1}$  in 2016 to  $0 \text{ g kWh}^{-1}$  in 2050. This constraint enables for the extent of  $\text{H}_2$  adoption to be clearly defined without the need for definition of demand scenarios and technology build-rate assumptions.

**3.1.6 Objective function.** The objective function is the total annualised cost (TAC) associated with meeting the demand for domestic and non-domestic heat. Eqn (6) denotes the objective function, which is minimised in the model formulation.

$$\begin{aligned} TAC = & CRF_j \sum_{tm} OW_{\text{CapEx},tm} TM_{\text{CapEx},tm} \\ & + \sum_{tm} OW_{\text{OpEx},tm} TM_{\text{OpEx},tm} \end{aligned} \quad (6)$$

where  $OW_{m,tm}$  is the objective weighting corresponding to each performance metric  $m$  at major time period  $tm$ ,  $CRF$  is the capital recovery factor and  $TM_{m,tm}$  is the total value of the performance metrics. Unless otherwise specified, the cost of capital used for transportation and storage infrastructure is 6%, with 14% assumed in the case of  $\text{H}_2$  production infrastructure.

### 3.2 Sensitivity analysis methods

The effects of uncertain model input parameters on the characteristics of the designed systems are studied using global sensitivity analysis (GSA) methods. Their usage has been argued by Keirstead and Shah<sup>68</sup> following the methodology outlined in Saltelli *et al.*<sup>69</sup> and has been implemented by Pye *et al.*<sup>70</sup> to solve similar design problems. In this paper, GSA is used in conjunction with the optimal design solution to determine the impact of 4 model input parameters: gas, electricity, biomass prices, and cavern costs, on the TAC of the designed system.

All four uncertain parameters are assumed to be uniformly distributed in the uncertainty space owing to a lack of reliable data to support the future distribution of parameter values. The resulting design solution is subjected to Monte Carlo simulations with a sample size of 10 000 simulations where the TAC from each simulation of the model is dependent on the parameter values that are generated at random from their respective probability distributions. Upon identifying relevant correlations, a multivariate linear regression model is developed using Ordinary Least Squares (OLS) regression to compare the relative importance of input parameters through measures such as the standardised regression coefficients. During this process, the regression model is assessed for its statistical significance, to ensure generality of findings and broader relevance. An elaborate description of the key statistical parameters that are used for assessing model and parameter fits can be found in Section S2 of the ESI.†

### 3.3 Modelling environment

The mathematical model is implemented and simulated in General Algebraic Modeling System (GAMS) version 25.0.3.<sup>71</sup>



Data processing for visualisation and analysis is conducted using Python version 2.7.<sup>72</sup> The geographical data is curated using the open-source Geographic Information System (GIS) tool: QGIS.<sup>73</sup>

## 4 Technology and resource needs in a low-carbon heat supply

The analyses presented in this section identifies the role of different H<sub>2</sub> production technologies in delivering varying levels of emissions reductions in the heating sector. Systemic trade-offs between technological options and storage are discussed in detail.

### 4.1 Which H<sub>2</sub> production technologies to deploy?

Fig. 5 illustrates the total installed capacity of production technologies at varying levels of CO<sub>2</sub> reduction. Each distinct scenario and its corresponding design optimisation was computed at a CO<sub>2</sub> reduction interval of 10%, ranging from 0% (complete inaction) to 100% (complete decarbonisation). The assumptions used to generate the outputs are summarised in Section S1 of the ESI<sup>†</sup> in addition to the key assumption that GB's cavern storage resources are usable. Similarly to previous contributions,<sup>74,75</sup> methane reforming pathways dominate the supply mix in all scenarios. This finding is in accordance with previous studies.<sup>74,75</sup> Owing to its superior energy efficiency and reduced costs of CO<sub>2</sub> avoidance, ATRs with GHR and CCS is the dominant technology choice under all emissions scenarios investigated.

Note the lack of deployment of technologies such as SMRs with fluegas capture, ATRs without GHR and the WE process. A comparison between the two ATR configurations on key performance metrics such as energy efficiency and levelised costs of H<sub>2</sub> production, render the configuration without GHR

as unfavourable. Although SMRs with fluegas capture have lower CapEx requirements than its ATR counterparts, this advantage is outweighed by a lower degree of economical CO<sub>2</sub> capture. This effect is compounded by benefits arising from higher output pressures that are achievable in ATRs as opposed to SMRs. Similarly, the WE process is not deployed in any of the scenarios due to its higher OpEx requirements (£63 per MW h of H<sub>2</sub> using an electricity price of £45 per MW h) compared to the reforming technologies (£18 per MW h of H<sub>2</sub> using a natural gas price of £13 per MW h). Furthermore, a CapEx reduction by 40% is necessary for the WE process to be comparable to ATRs.

Large scale availability of biomass may enable gas-reliant nations to achieve net-zero emissions from a H<sub>2</sub>-based heating supply through the combination of ATRs and BG with CCS.<sup>76,77</sup> In fact, under the assumptions of this study, the maximum achievable reduction in CO<sub>2</sub> emissions without the use of biomass is 85%. A key problem, which is largely unaddressed in literature, relates to the effect of variable CO<sub>2</sub> capture rates on the cost competitiveness of fossil-based production facilities compared to NETs. The possibility to achieve greater CO<sub>2</sub> removal by increasing the capture rates beyond 90% for CCS facilities is accompanied with very low marginal costs in the case of power generation facilities.<sup>78</sup> However, further research must be undertaken to establish the economic value in raising the capture rates beyond 94% in ATRs. Furthermore, a comparison between the different NET options to provide negative emissions services can identify cost-effective opportunities.<sup>79</sup>

At lower CO<sub>2</sub> removal targets, natural gas is used as the principal heating fuel with ATRs dispensing H<sub>2</sub> in favourable locations to achieve lower overall total system costs. In addition to the ATRs, SMRs with syngas capture contribute significantly towards overall H<sub>2</sub> supply as evidenced by almost 14 GW of capacity *via* this technology under a CO<sub>2</sub> reduction level of 50%. Its economic favourability is the largest driver influencing its deployment. Nevertheless, this technology does not make any contributions to the design capacity at higher CO<sub>2</sub> removal targets due to its greater CO<sub>2</sub> footprint.

It is important to note that the maximum design capacity across all scenarios is approximately 55 GW. Current estimates of total UK H<sub>2</sub> production capacity varies between 3–5 GW based on capacity factors of 70–90% at an annual throughput of 27 TW h.<sup>49</sup> Thus, the design capacity is at least an order of magnitude larger than existing capacity. This signifies the importance of technologies such as ATRs with CCS, which can be deployed in larger capacities (at GW scales) as opposed to options such as WE or BG with CCS, requiring significant scale-up before deployment. Additionally, the design capacity is equivalent to a quarter of the estimated peak hourly domestic demand of 205 GW, implying an extensive network reliance on large scale underground H<sub>2</sub> storage.

### 4.2 Economic trade-offs between H<sub>2</sub> production and storage infrastructure

The system value of storage availability in a time dependent application such as heating consumption is illustrated in Fig. 6. The system value, in this instance, is defined as the reduction

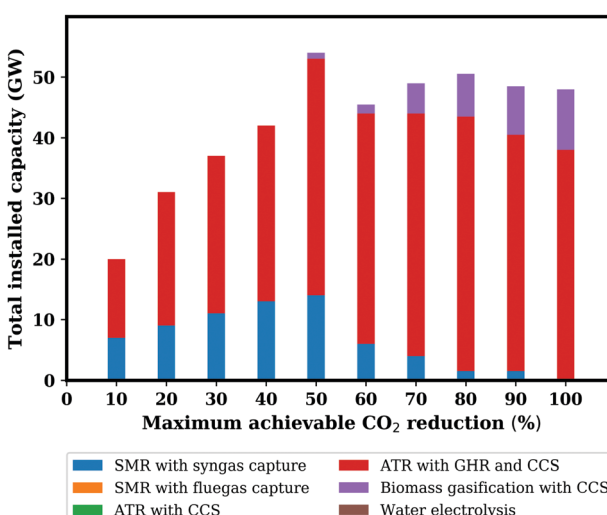


Fig. 5 The optimal mix of technologies deployed in distinct designs show the extent to which the decarbonisation targets influence the nature of the overall design capacity.



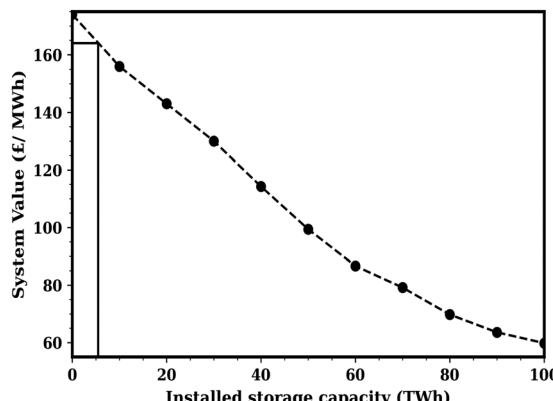


Fig. 6 System value of  $\text{H}_2$  storage in a net zero emissions based heating supply as a function of installed storage capacity. The system value is quantified based on a reduction in TAC, relative to a supply with no storage. The polygon in the left of the figure represents the value of the existing storage potential in GB if natural gas caverns were repurposed to store  $\text{H}_2$ .<sup>80</sup>

in TAC per unit of storage installed.<sup>81</sup> The curve indicates the potential for diminishing returns with increases in available storage volume. Thus, expansion of available storage through construction of additional caverns can add limited value to the system. An approximate twelve-fold increase in  $\text{H}_2$  storage capacity to 65 TW h within GB offers a 20% reduction in TAC compared to that in the absence of any storage. Importantly, the ability of production technologies to satisfy varying demands in regions without geological storage is not very well understood. The optimal technology choices from Section 4.1 may not necessarily be applicable in the absence of sufficient storage. The total design capacity requirements for a complete decarbonisation of demand with increasing availability of storage potential is depicted in Fig. 7.

Owing to economies of scale, reforming technologies at lower sizes (400 and 700 MW) are not deployed at all under storage limitations. The WE process appears to be dominant in the complete absence of storage infrastructure although it is only utilised at peak demands due to its higher OpEx requirements. The peak day operating mix in the complete absence of storage is summarised in Section S3 of the ESI.† In general, the deployment potential of the WE process does not rely on storage availability as direct access to grid power can tackle the intermittency of renewable sources. Nevertheless, there appears to be an economic incentive to deploy this technology at scale due to its favourable ability to respond rapidly to load variations. A corollary of the above observation is that the value of flexible production in technologies is increased in storage-constrained applications. The total design capacities of both ATRs and BGs with CCS are largely invariant and independent of the amount of available storage. These technologies can be utilised to a greater extent throughout the annual time horizon.

From Fig. 7, it also appears favourable to install SMRs with syngas capture in regions with limited access to storage infrastructure. The provision of storage infrastructure enables the inflexible reformer units to operate at higher utilisation

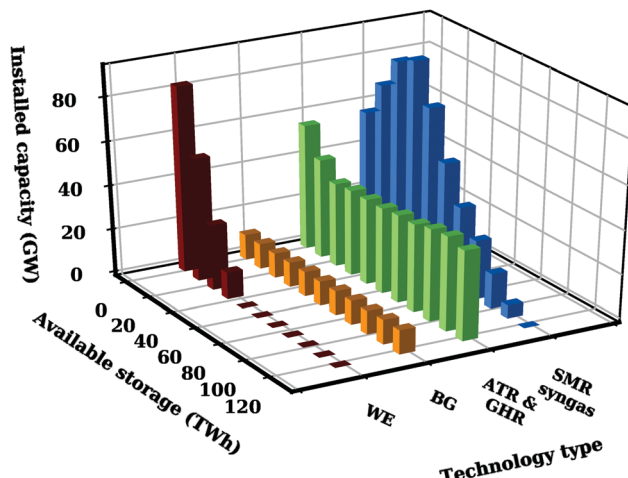


Fig. 7 Total installed capacity of the individual production technologies with varying  $\text{H}_2$  storage potential. Technology label WE: water electrolysis, BG: biomass gasification with CCS, ATR & GHR: autothermal reforming with gas heating reforming and CCS, SMR syngas: steam methane reforming with syngas  $\text{CO}_2$  capture. It is important to note here that both WE and  $\text{H}_2$  storage are in competition for providing resilience to the system. In particular, there needs to be a significant deployment of WE if no additional  $\text{H}_2$  storage is developed.

rates without the need for significant operational flexibility. SMRs with syngas capture are only utilised in periods of high demand even though their aggregate design capacity is higher than the remaining options. Negative emissions are provided via BG with CCS and used to offset the residual emissions from SMR with syngas capture.

#### 4.3 What is the impact on resource consumption?

The annual resource consumption requirements were computed as an aggregate of the resource usage across all of the production technologies in the capacity mix. The power requirement across all production processes was translated into further natural gas consumption through the definition of an average conversion efficiency of 44% for the electricity grid, which is representative of the UK as reported by the IEA.<sup>82</sup>

Fig. 8 displays the resource requirements for natural gas and biomass at varying levels of decarbonisation. Due to the favourable deployment of reforming technologies with CCS, natural gas continues to have significant importance in a low-carbon environment. Its consumption can be expected to increase in designs with achievable system-wide emissions reduction of 60% or below as illustrated by the figure. However, further reductions in  $\text{CO}_2$  emissions result in the consumption of biomass, which reduces the overall consumption of natural gas to figures comparable to present use. Therefore, it can be clearly stated that a least cost supply of  $\text{H}_2$  does not necessarily increase the national reliance on natural gas, especially if  $\text{CO}_2$ -neutrality is the principal design constraint. The energy conversion efficiency, expressed as the share of energy output relative to the energy input for the heat supply, ranges from 58% (net-zero emissions using  $\text{H}_2$ )–92% (natural gas). The adoption of a least cost network for complete decarbonisation



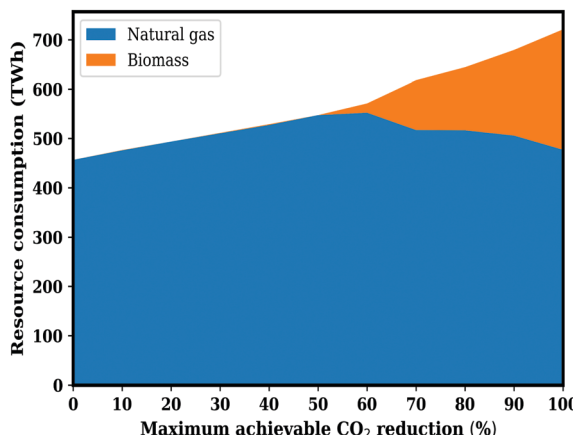


Fig. 8 Total primary resource consumption for GB at varying levels of CO<sub>2</sub> reduction, demonstrating the increasing slope in energy consumption at higher decarbonisation targets with current consumption highlighted at a CO<sub>2</sub> reduction level of 0%.

appears to reduce the total resource conversion efficiency. This is primarily due to the increasing deployment of BG with CCS, which is less energetically efficient compared to the methane reforming routes, and direct combustion of natural gas. Improvements in the energy efficiency of NETs will support a resource efficient, sustainable transition into a net zero emissions-based H<sub>2</sub> economy.

## 5 Regional transition pathway

### 5.1 Rate of deployment

By 2050, 48 GW of H<sub>2</sub> production capacity (40 GW from ATRs with GHR and CCS and 8 GW from BG with CCS), which is at least an order of magnitude increase compared to present capacity, needs to be installed with large scale expansions in storage infrastructure. BG with CCS needs to be introduced as early as 2020s for cost-effective reduction in CO<sub>2</sub> emissions. The rate of deployment of production capacity is greater in the first ten years of the transition (1.6 GW per year) than at later times (1.1 GW per year). The rate of development of storage assets across the Cheshire, East Irish Sea, East Yorkshire within GB is approximately linear at 1.7 TW h per year. Within the first 5 years of the transition, the total storage capacity developed for H<sub>2</sub> is approximately equivalent to existing natural gas storage volume within GB. The rate of deployment of storage infrastructure increases to 3.7 TW h per year through the installation of caverns in the Dorset region from 2035 onwards. The infrastructure eventually relies on approximately 85 TW h of cavern-based H<sub>2</sub> storage by 2050, which is within GB's capabilities.<sup>83</sup> As a result, there is an increase in the relative share of investment that is apportioned to H<sub>2</sub> storage with time.

The maximum amount of CO<sub>2</sub> injection capacity needed by 2050 is approximately 105 Mt per year (30 Mt per year in the East Irish Sea, 65 Mt per year in the Southern North Sea, and 9 Mt per year in the Northern North Sea). The overall requirements for CO<sub>2</sub> storage in the North Sea over the 35 year lifetime

of H<sub>2</sub>-based heating infrastructure is approximately 3.7 Gt CO<sub>2</sub>, which is within GB's capabilities based on injection rates between 1–2.5 Mt per year per well as shown in Mathias *et al.*<sup>56</sup> and Bentham *et al.*<sup>84</sup> The average rate of development of CO<sub>2</sub> storage capacity is 3.1 Mt per year, which is particularly challenging given that at the time of writing, there are no operational CO<sub>2</sub> storage projects within the region.

The absence of a commercially viable business model presently hinders the deployment of CCS infrastructure. Governments have an important role in reframing the policy initiatives to encourage investment in CCS technology. CCS supply chains are technically and commercially mature, unlike several other low-carbon technologies, and are well suited to large-scale applications as demonstrated through an array of projects.<sup>85</sup> The urgent need to deploy infrastructure, as highlighted by this study, limits the capacity for new and immature technologies to have a material impact. In the absence of government intervention and the formulation of suitable business models, nations could expose themselves to the risk of failing to meet carbon-neutrality due to the increasing strains on immature, new technologies.

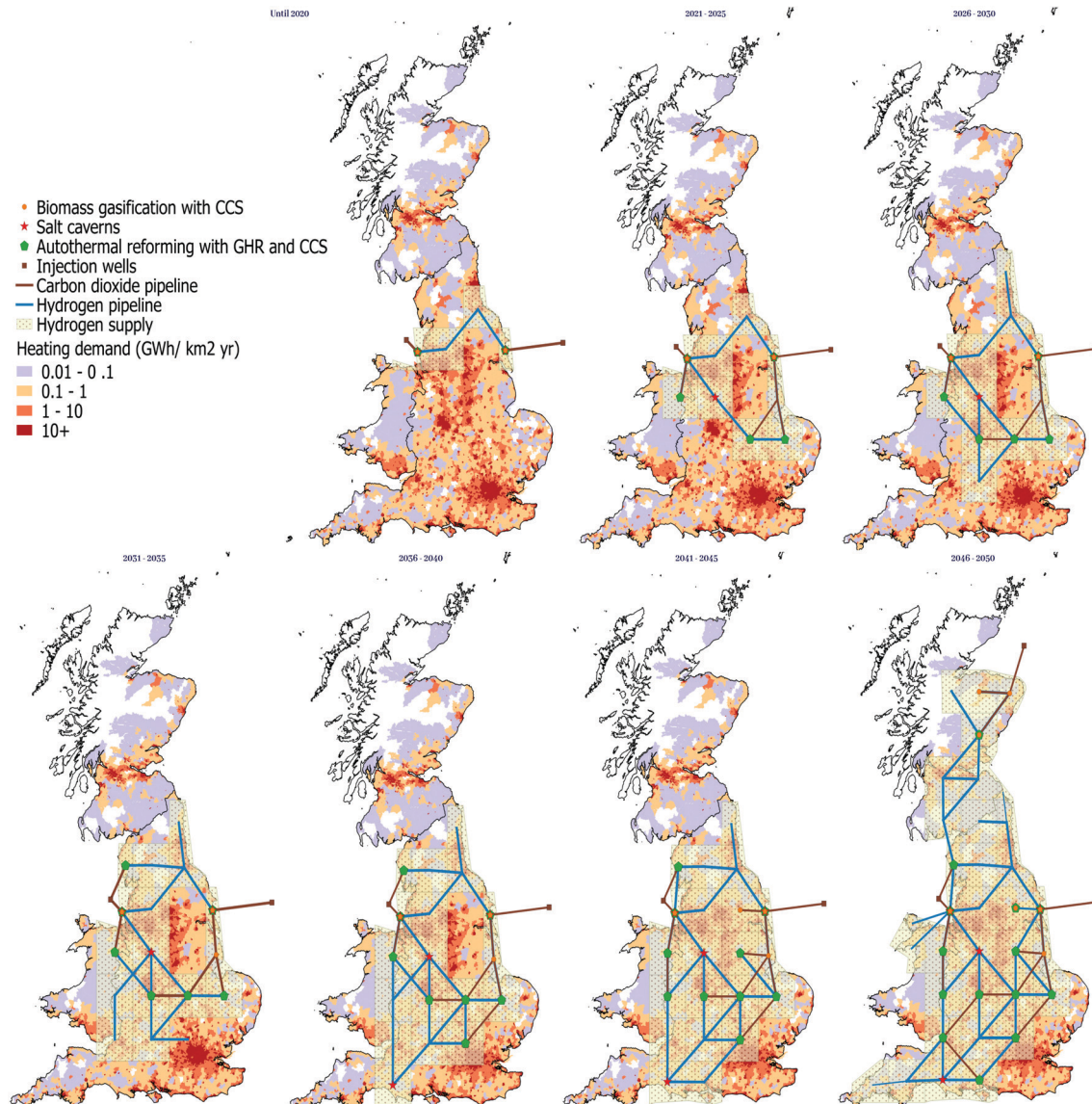
### 5.2 Cost-optimal regions

Fig. 9 depicts the regional deployment trajectory to support the complete decarbonisation of the heating sector. By 2020, approximately 10 GW of H<sub>2</sub> production capacity is distributed over two locations, representing the centralised nature of production. Production technologies are located in coastal regions with access to H<sub>2</sub> storage in addition to close proximity to CO<sub>2</sub> storage. The total demand for H<sub>2</sub> in adjoining regions appears to have an influence on optimal infrastructural locations, but to a lesser extent than the aforementioned factors. Nevertheless, the cumulative production capacity installed in a given location is dependent on the scale of demand in conjunction with availability of H<sub>2</sub> storage.

During the expansion process, network connectivity appears to be maintained between production facilities through the emergence of H<sub>2</sub> transmission pipelines. This is not necessitated by the model constraints, which enforce an aggregate rather than a regional reduction in the CO<sub>2</sub> emissions. An alternative mode of expansion could involve the conversion of fuel supply in a completely distinct region in which all of its adjoining neighbours are supplied with natural gas. Naturally, H<sub>2</sub> production technologies must be installed in such a region. However, such possibilities are not realised in the optimal deployment trajectory, displaying economic benefits arising from a well connected network, potentially due to a greater utilisation of economic benefits arising from an asymmetric distribution of production capacity across a geographical region.

### 5.3 H<sub>2</sub> storage is a network driver

In Fig. 9, there exists a sub-region (surrounded by the dotted region in the North East of England) which uses natural gas whilst all of its neighbouring regions utilise H<sub>2</sub>, forming a regional enclosure. This might not constitute a practicable conversion as it is difficult to isolate gas distribution supply.



**Fig. 9** Illustration of the investment locations and the deployment trajectory for infrastructural components at 5 year time intervals to achieve net-zero CO<sub>2</sub> emissions over a 35 year time horizon. The first investments in H<sub>2</sub> production and storage infrastructure are concentrated in the North of England, with CO<sub>2</sub> storage in both the East Irish Sea and the Southern North Sea. Further expansions in infrastructure utilise available volumes of H<sub>2</sub> storage to support the deployment of ATRs and BGs. H<sub>2</sub> is dispensed to areas with lower heating demands at the later phases of the transition as these regions are less economical.

The gas supply in this region is only converted to H<sub>2</sub> during 2040–2045 even though the region has high demands in addition to CO<sub>2</sub> storage and H<sub>2</sub> storage. Note that approximately 43% of GB's total H<sub>2</sub> cavern storage potential is located in the three sites developed by 2025. This share is equivalent to 38 TW h of which 21 TW h is utilised by 2025. It is important to delineate this data as fuel switching from natural gas to H<sub>2</sub> in the enclosed region would entail a near complete utilisation of the remaining 17 TW h of cavern storage potential. If converted initially, further regional expansions cannot utilise cavern storage without the integration of storage potential from the Dorset region (southernmost region with caverns). In such instances, the demand must be satisfied wholly through increases in production capacity, resulting

in increased costs during expansion, which can be mitigated by the delayed conversion of the enclosed region. This is evidenced by the continued expansion of H<sub>2</sub> network to the southern regions incorporating localised areas of high demands in addition to the development of storage infrastructure in the Dorset region by 2040. Further network expansions during 2041–2045 finally convert the aforementioned enclosed region. This emphasises the importance of H<sub>2</sub> storage availability on the deployment rates of infrastructure and its overall utilisation for cost-effective decarbonisation.

#### 5.4 Low demand areas are more expensive

By 2050, the network extends further to regions within Scotland, resulting in a completely decarbonised heating network. The delayed



conversion of Scotland stems from the increased expenditures that are incurred to satisfy a relatively sparse distribution of demand, although the absence of cavern storage is likely to be a factor of greater importance. A near complete conversion of Scotland's gas supply may not be practicable in 5 years due to the large extent of geographical areas that are involved. This is an outcome of the assumptions related to a linear reduction in emissions across the heating sector. The results indicate that localised regions with high heating demand densities are converted with priority since they offer substantial reductions in CO<sub>2</sub> emissions intensity without incurring additional costs for transmission infrastructure. Thus, regions with low heating demand densities are converted only if higher levels of CO<sub>2</sub> reduction are desired. A complete conversion of regional gas supply to H<sub>2</sub> is not necessary for complete decarbonisation of the heating network. This is principally due to the availability of biomass for providing negative emissions services, enabling the continued use of natural gas in regions where it is economically unfavourable to supply with H<sub>2</sub>.

## 6 Economic evaluation

### 6.1 Capital investment breakdown

The key components of infrastructure CapEx are structured into different functional categories such as Production, Transportation, Compression and Storage with relative CapEx shares of 27%, 11%, 1% and 61% respectively as illustrated *via* Fig. 10. Note that the transport investments for H<sub>2</sub> specifically refer to transmission infrastructure as opposed to distribution infrastructure. The latter is assumed to be available as a result of the conversion of cast iron pipelines through the Iron Mains Replacement Programme (IMRP) in the UK.<sup>86</sup>

The total investments within each category are evaluated as an aggregate sum total of the infrastructural investments across the entirety of the system. The "Production" category contains

all the investment costs associated with H<sub>2</sub> production with integrated CO<sub>2</sub> capture, in addition to equipment costs for compression, purification of H<sub>2</sub> and CO<sub>2</sub> within the battery limits of the installed plant. When technologies such as ATRs are used, total investment costs include Air Separation Unit (ASU) installation costs. The "Transportation" category contains infrastructural investments required for H<sub>2</sub> and CO<sub>2</sub> piping both onshore and offshore. The "Compression" category contains capital requirements for the installation of "booster" or intermediate compression stages across the length of a pipeline, when necessary. Finally, the "Storage" category contains the investment costs associated with the installation of underground H<sub>2</sub> storage as well as CO<sub>2</sub> storage. The largest cost component across the entire system is H<sub>2</sub> storage which surpasses production related investments, providing greater economic value than what is achievable in its absence. ATR facilities contribute more towards production-related investments than BG with CCS due to its greater share of installation capacities. Overall transportation costs are higher for H<sub>2</sub> compared to CO<sub>2</sub> due to the larger pipeline network. The availability of distribution infrastructure lowers the overall investment requirements considerably as the low-pressure distribution network (218 000 km) is much larger than the high-pressure transmission network (19 600 km) for natural gas.<sup>13</sup>

The transition pathway presented in this study relies on the retirement of the first production assets with CCS in the period between 2050–2060. By that time frame, improvements in water electrolysis technology along with potentially lower electricity costs could enable a low-cost transition to an electrolytic-H<sub>2</sub> supply. As noted above, the investment requirement for production infrastructure is 27% of the total investment capital, representing a smaller share in comparison with H<sub>2</sub> storage and transmission infrastructure. The infrastructure investments are also necessary for electrolytic-H<sub>2</sub> production due to the intermittency of renewable power. Furthermore, any unused CO<sub>2</sub> transport and storage infrastructure can be used to facilitate industrial CCS and negative emissions technologies, thereby improving the robustness of infrastructure investments.

### 6.2 Impact of the cost of capital

The total costs associated with a transition into a H<sub>2</sub>-based heating sector is greatly influenced by the cost of capital. The sourcing of capital for funding this enterprise remains a key challenge. Fuel poverty remains a major issue in several gas-reliant nations and potential infrastructural changes must avoid exacerbating these issues and ensure affordable access to energy services. Government financing from its generated revenue was used for gas infrastructure financing in the transition from a town gas-based heating network to natural gas in GB by 1970s.<sup>87</sup> Although government ownership has the ability to lower the project costs compared with private financing, the procurement of necessary funding may have significant impacts on consumers' purchasing power. Alternative financing strategies could seek involvement from the private sector for financing some or all of infrastructural operations in the network. However, private sector investment is unlikely to

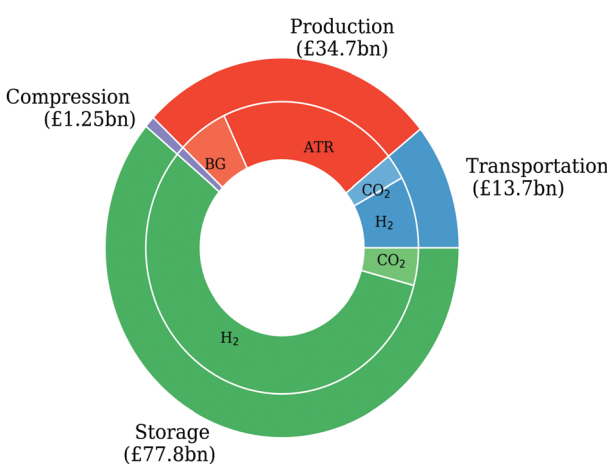


Fig. 10 An illustration of the total CapEx breakdown over different system components, indicating the highly capital-intensive nature of infrastructure investment. The cost of capital for transport and storage infrastructure is 6%, whereas it is 14% for production infrastructure. H<sub>2</sub> storage is the largest component of total CapEx.



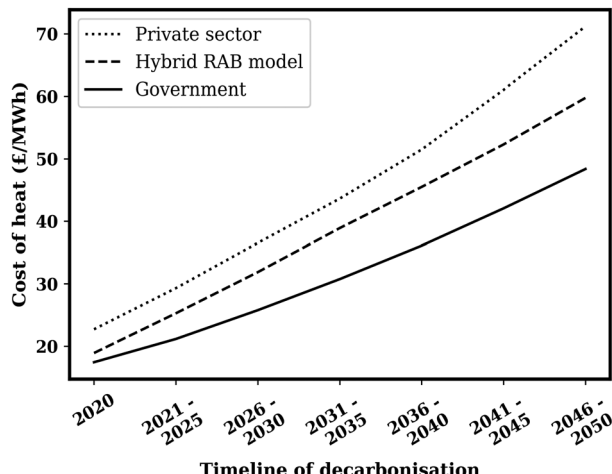


Fig. 11 The total cost of heat supply for consumers through different business models. Note that supplier margins and distribution-related costs are not included in these estimates and will influence the final cost of heat delivered for the consumer. The cost of capital assumed for government and private sector investment are 3.5% and 14% respectively. The hybrid RAB model assumes a cost of capital of 6% for transport and storage elements and 14% for production infrastructure.

materialise without long-term assurances and a revenue certainty from market operations.

The total costs associated with the supply of heat calculated for three distinct scenarios, are shown in Fig. 11. The distinctions indicate the effect of financing *via* (a) private sector financing in its entirety; (b) hybrid regulated asset base (RAB) framework,<sup>88</sup> with a lower cost of capital for transport & storage of both H<sub>2</sub> and CO<sub>2</sub> elements, along with private sector financing rates for the production infrastructure; (c) government financing in its entirety. For the private sector scenario, a cost of capital of 14% was assumed. The hybrid RAB model for transport & storage assumes a cost of capital of 6%,<sup>89</sup> with private sector hurdle rates for production infrastructure. The government cost of borrowing was assumed to be 3.5%<sup>90</sup> and in all these scenarios, an economic lifetime of 35 years was assumed. Fig. 11 shows the evolution of the cost of heat for consumers depending on the commercial frameworks that are deployed. By 2050, the cost of heat can be estimated as £48 per MW h, £60 per MW h and £71 per MW h under government, hybrid RAB and private sector cost structures respectively. This reflects cost increases of 190%, 260% and 320% relative to heat from natural gas, thus increasing the potential for more consumers to be “fuel poor” in the absence of any financial support. Nevertheless, the hybrid RAB model may prove to be important in mobilising investment through the reduction of risk (relative to private finance), thereby improving the affordability of the infrastructure.

### 6.3 Cost of heat supply

GSA is used based on the methodology summarised in Section 3.2 to evaluate the variability in the cost of heat supply, and derive insights into the likely level of financial support required to deploy infrastructure. 4 model parameters were selected for

sensitivity analysis: gas, electricity and biomass prices in addition to cavern cost as they represent key uncertainties. The uncertainty intervals for gas and electricity price distributions are based on the projections by BEIS on future prices.<sup>13,91</sup> Similarly, the intervals for biomass price are captured from Committee on Climate Change (CCC) projections of future prices.<sup>92</sup> Cavern costs may vary depending on the sites and their specific construction and operation requirements. Intervals for cavern costs were conservatively chosen based on estimates of low and high cost thresholds, capturing evidence from recent technical appraisals.<sup>9,13,53</sup> 10 000 samples were subsequently generated from a uniform distribution of the input parameters and simulated to evaluate their impact on the TAC.

Multivariate linear regression was used to identify  $\beta$  coefficients that rank the relative importance of these input parameters as first order sensitivity indices. The estimation procedure adopted for the formulation of the regression model involved identifying the input parameters with largest correlation on the output. The adjusted coefficient of determination,  $\bar{R}^2$  modifies  $R^2$  based on the number of independent variables and the sample size to ensure that overfitting of the data is avoided. Section S2 of the ESI† contains detailed equations for  $\bar{R}^2$  and  $\beta$  coefficients. The simplest model form containing gas price as the sole explanatory variable results in a  $\bar{R}^2$  value of 0.505. The inclusion of biomass price and subsequently, cavern costs increase the  $\bar{R}^2$  value to 0.768 and 0.984 respectively. This leads to the conclusion that almost all of the variance in the cost of heat supply stem from the potential variability in gas, biomass prices in addition to cavern costs. The  $\beta$  coefficients for gas price, biomass price and cavern cost are 0.71, 0.51 and 0.47 respectively. This exposes gas price as the factor of greatest impact on the cost, followed by the biomass price and CapEx of caverns. Further details on the statistical validity of the regression models and corresponding  $\beta$  coefficients are described in Section S3 of the ESI.†

The total costs of CO<sub>2</sub> avoidance was obtained by normalising the output TAC vector by the CO<sub>2</sub> emissions avoided in the design. Fig. 12 illustrates the distribution of the aforementioned metric using histograms with a bin width of 0.25. The resulting data approximates a normal distribution with a mean of £176 per ton and a standard deviation of £18 per ton. The distribution covers an interval ranging between £120–240 per ton. The levelised costs of a H<sub>2</sub>-based heat supply under a hybrid RAB model ranges between 5.2–8.6 pence per kW h compared to natural gas at 1.0–2.8 pence per kW h based on the guidance from BEIS.<sup>13,91</sup> Over a 35 year timeframe, the total cost of heat supply may be greater by a factor of 3 on average compared to present prices.<sup>94</sup>

There is a policy gap in the domestic and commercial heating sectors in the majority of countries, which pertain to the usage of unabated natural gas without any economic penalties. The development of market reforms with appropriate levers, such as the introduction of an effective CO<sub>2</sub> price, on unabated natural gas consumption will be necessary in the long-term. However, a complete reliance on a free-market



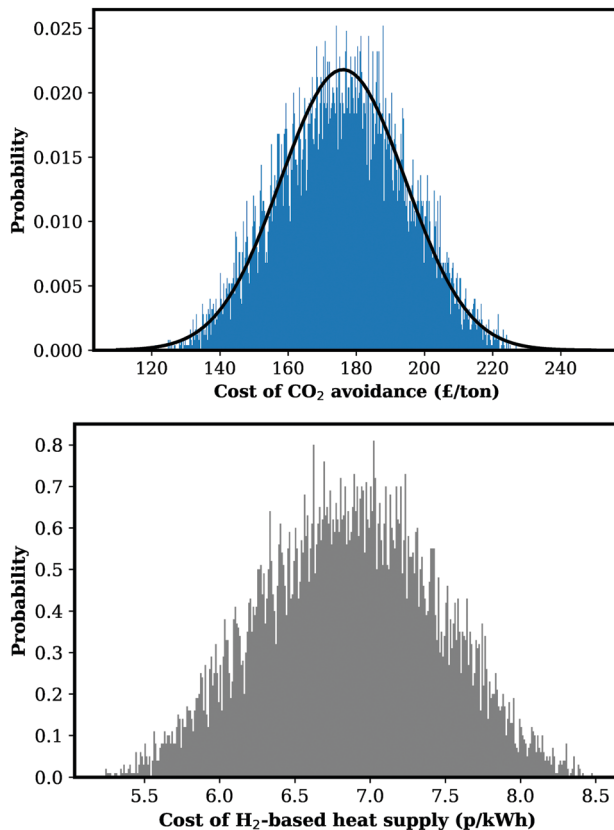


Fig. 12 The total cost of CO<sub>2</sub> avoidance, and heat supply as a result of deploying H<sub>2</sub>-CCS infrastructure in 2050. The cost of heat supply excludes distribution-related charges, which is typically responsible for 25% of a domestic natural gas bill.<sup>93</sup> The relative contribution of distribution related costs to the overall cost of H<sub>2</sub>-derived heat is likely to be lower compared to natural gas. Nevertheless, the cost of a H<sub>2</sub>-based heat supply is on average, three times more expensive than natural gas at present.

approach without any financial support is likely to be undesirable, even with an active CO<sub>2</sub> emissions trading market in the aforementioned sectors. This is especially the case if the CO<sub>2</sub> price floor is insufficient to encourage investment, resulting in a delayed start to the energy transition. This precipitates the need for higher rates of technology deployment in later years in order to achieve net-zero emissions, thereby increasing the risk for supply chains and potentially compromising the transition. Therefore, financial support mechanisms are likely to be necessary in facilitating investment in low-carbon H<sub>2</sub> production assets.

An appropriate level of financial support for a mechanism such as a Contract for Difference (CfD) was estimated by costing the production infrastructure at a cost of capital of 14%, which is typically used by the private sector. This results in a strike price for the heat service, ranging between £40 per MW h and £67 per MW h. Assuming the cost of natural gas supply as the market price for the heat service, a CfD payment between £20 per MW h and £53 per MW h may be necessary for H<sub>2</sub> producers alone. Additionally, a CO<sub>2</sub> price of £104–£268 per ton is necessary in order for H<sub>2</sub> to achieve parity relative to natural gas without any financial support.

Thus, higher market valuations of the externalities associated with CO<sub>2</sub> will ensure that methane-derived H<sub>2</sub> supply can operate independently without the need for ongoing financial subsidies. The cost of the remaining RAB for transport and storage elements amounts to £11–£18 per MW h as opposed to £19–£32 per MW h, which would be required *via* the private sector in the absence of a regulated framework. It is possible to reduce the overall cost of heat supply by securing natural gas and biomass supply contracts under approximately £17 per MW h and £90 per ton. Technology appraisals in cavern construction and operation will also lead to uncertainty reduction in the estimates for total costs. In addition, the efficient management of resource supply chains can reduce the total costs considerably as summarised in Section S3 of the ESL.<sup>†</sup>

Additional revenue from carbon capture and utilisation (CCU) can improve the economic viability of infrastructure investments. However, the overall global warming potential of the CCU process must be considered, along with the end-use market for CO<sub>2</sub>-derived products on a case-by-case basis. New advancements in CO<sub>2</sub> capture materials, solvents and processes have the ability to lower the cost of CO<sub>2</sub> abatement *via* both ATRs and gasification.<sup>95</sup> However, further economic analysis must be undertaken to identify the most suitable materials for large-scale applications. Furthermore, recent developments in photocatalytic water splitting have shown the potential to operate at higher efficiencies than commercially available electrolysis technology.<sup>96</sup> Similarly, Chen *et al.*<sup>97</sup> has shown that the electro-oxidation of biomass-derived alcohols have the ability to lower the overall energy requirements relative to conventional WE. Nevertheless, additional research and development efforts are needed to increase the technology readiness levels of these technologies towards commercialisation.

## 7 Conclusion

ATRs with GHR and CCS have an important role (75–80% of the installed capacity) due to their ability to provide cost-effective CO<sub>2</sub> mitigation. The deployment of larger capacity modules are preferable in regions with high demands due to economies of scale effects. A low-carbon H<sub>2</sub>-based heat supply can be developed cost-effectively through the deployment of reforming technologies with CCS and NETs using large scale H<sub>2</sub> storage in salt caverns, and CO<sub>2</sub> storage in deep geological reservoirs. The exact technology portfolio is likely to differ depending on the analysed region, based on spatio-temporal variations in H<sub>2</sub> demand, geological storage, *etc.*

It was found that a ten-fold expansion in H<sub>2</sub> storage capacity to approximately 65 TW h could yield a reduction in total system costs by at least 20% relative to a system with no H<sub>2</sub> storage. Both WE and H<sub>2</sub> storage compete to provide resilience and flexibility to the designed infrastructure. The WE process is primarily deployed in the absence of H<sub>2</sub> storage as a process for satisfying peak demands. Thus, displaying parallels with the usage of back-up fossil generation in the power sector for meeting peak demands.



The overall energy conversion efficiency of heat supply decreases from 92% (natural gas) to 58% (net-zero emissions using H<sub>2</sub>), when considering all the infrastructural operations from the battery limit of the production plant to the use. This is mainly due to the lower resource efficiency of key technologies such as BG with CCS. A complete regional conversion of natural gas supply to H<sub>2</sub> is unnecessary for net-zero CO<sub>2</sub> emissions due to the availability of NETs. Cost-effective regions for locating infrastructure are distinguished by their relatively high demands for H<sub>2</sub> in addition to storage availability for both H<sub>2</sub> and CO<sub>2</sub>. HSCs that are based on methane reforming technologies may necessitate local reinforcements to existing natural gas transmission infrastructure to manage the increased load requirements from the production facilities. Furthermore, cost-optimal regional transitions to a H<sub>2</sub>-based heat supply exploits network connectivity through H<sub>2</sub> pipelines. This indicates that it is economically favourable to centralise H<sub>2</sub> production and expand from existing infrastructure than have a distributed mode of production. These findings imply that cost-effective transitions into H<sub>2</sub>-CO<sub>2</sub> infrastructure in other geographies are dependent on the identification of similar regional characteristics.

Total investment capital requirements are contingent on the CapEx of H<sub>2</sub> storage infrastructure in addition to the production infrastructure. Transportation infrastructure for both H<sub>2</sub> and CO<sub>2</sub> contribute a relatively smaller share (11%) towards total investment requirements. Total system costs, comprising of both investment and operation elements, is mostly influenced by the natural gas price, followed by biomass price and cavern construction costs. The total cost of CO<sub>2</sub> avoidance was closely approximated by a normal distribution with a mean of £176 per ton and a standard deviation of £18 per ton. The levelised cost of a H<sub>2</sub>-based heat supply ranges between 5.2–8.6 pence per kW h compared to a natural gas supply at 1.1–2.8 pence per kW h.<sup>91</sup> Over the lifetime of the infrastructure, the total cost of heat supply may be greater by a factor of 3 on average compared to present prices. A financial support mechanism such as a CfD payment of £20–£53 per MW h is necessary for H<sub>2</sub> producers in order to achieve price parity with natural gas until an effective CO<sub>2</sub> price of £104–£268 per ton is reached, thereby eliminating the need for support. Furthermore, a hybrid RAB model reduces the cost contribution of transport and storage elements from £19–£32 per MW h to £11–£18 per MW h, resulting in a more affordable energy transition for the consumer. Importantly, comparable levels of financial support are likely to be required for the transition to occur in other regions, especially as natural gas is cheaper than H<sub>2</sub> at present.

The authors note that improvements in technologies and the resource market have the potential to influence the specific infrastructural solution. However, a key insight from this study is that the high deployment rates required for carbon-neutrality by 2050 necessitates prompt action. There is insufficient time to innovate and scale-up new technologies in the period to 2050, especially as the deployment pathway is challenging to achieve with readily available technologies, which have established supply chains. Future work should analyse the role

of H<sub>2</sub> in tandem with other CO<sub>2</sub> abatement options to better understand their influence on infrastructure planning, policy frameworks and regional productivity.

## Conflicts of interest

There are no conflicts to declare.

## Appendices

### A Resource and technology characterisation

**A.1 Resources.** Resources in this formulation describe primary feedstocks and intermediates (*i.e.*, natural gas, biomass, *etc.*) and energy vectors (H<sub>2</sub>, electricity). These resources are interconverted by process technologies, transported from one cell to another, imported, stored or retrieved at every time period in the planning horizon. Defining a complete set of feedstocks is a useful concept from a planning perspective as it becomes possible to design additional infrastructure for the feedstocks and intermediary resources in addition to the products when viable. A description of maximum import rates for importable resources is not included as it is likely that existing infrastructure (*e.g.*, gas processing terminals) will require expansion to support a low-carbon H<sub>2</sub> network.

The pressure levels of resources such as H<sub>2</sub> and CO<sub>2</sub> in pipelines are modelled through a discrete representation of pressure. Maximum mass flowrates in pipe flow are computed on the basis of average pipeline length (*i.e.*, identical to the cell distance), its sizing dimensions and maximum allowable pressure drops. The process modelling software, gPROMS was used to perform pressure drop calculations using Haaland and constant friction factor correlations.<sup>98</sup> Physical property data for H<sub>2</sub> was obtained using the gSAFT- $\gamma$  Mie component package with the exception of the fluid viscosity term, which was obtained from the National Institute of Standards and Technology (NIST).<sup>55</sup> Maximum allowable pressure drops were determined by ensuring that the flow velocity does not exceed the erosional velocity in pipelines. The maximum flow capacity was constrained on the basis of maximum allowable flow velocity and corresponding pressure drops through pipelines of distinct sizes. Consequently, H<sub>2</sub> transmission pipelines were constrained on the basis of a peak pressure drop of 20 bar across its pipeline length (approximately 80–100 km). This description enables the computation of investment decisions associated with intermediate compressor stations spaced along the pipeline. Pressure drops for CO<sub>2</sub> were evaluated at a range of desired flowrates and pipeline lengths, leading to the observation that it is not a constraining factor. Thus, “booster” stations were not explicitly taken into account for dense phase CO<sub>2</sub>.

**A.2 Production technologies.** In this study, production pathways incorporate CCS and considers steam methane reforming (SMR), auto-thermal reforming (ATR), ATR with gas heating reforming (GHR) and biomass gasification (BG). In addition, the water electrolysis (WE) process using Proton Exchange Membrane (PEM) electrolyzers is also included.



Multiple plant configurations of SMRs with CCS are explicitly considered to evaluate its overall deployment potential. All production technologies using natural gas are assumed to use the National Transmission System (NTS). Similarly, all technologies using electricity are assumed to use power from the national grid. Total sustainable UK biomass potential in 2050 was estimated to range between 200–550 TW h p.a. by the CCC, increasing from approximately 145 TW h.<sup>92</sup> Liquid H<sub>2</sub> production is not considered and all production facilities are assumed to be capable of delivering H<sub>2</sub> at purities in excess of 99%.

**A.2.1 Steam methane reforming (SMR).** The SMR process is undoubtedly the most mature and dominant process technology for the production of H<sub>2</sub>.<sup>99</sup> Approximately half of global H<sub>2</sub> supply is produced using this process<sup>100</sup> in view of its attractive economical performance.<sup>101</sup> The process uses a pre-heated feed of methane and steam which reacts in a reformer unit to produce a syngas mixture containing CO, CO<sub>2</sub> and H<sub>2</sub>. The syngas mixture undergoes further conversion with steam in the water gas shift (WGS) reactor in order to produce more H<sub>2</sub>; this process is accompanied by a further conversion of CO into CO<sub>2</sub>. The reforming reactions are highly endothermic and require a significant supply of heat. This process typically operates at 800–1000 °C and at pressures of 20–40 bar. The effluent stream undergoes purification using technologies such as Pressure Swing Adsorption (PSA) in order to remove CO, CO<sub>2</sub> and H<sub>2</sub>O. There are two key sources of emissions in this process: (a) from the conversion of methane/CO with steam; (b) from the combustion of methane as a fuel.

Two potential plant configurations with CCS were considered promising for cost-effective CO<sub>2</sub> capture from the analysis presented by Amec Foster Wheeler and the International Energy Agency (IEA).<sup>43</sup> Amine based absorption technologies can be integrated with the SMR process to capture CO<sub>2</sub> from the syngas stream to remove 55% of all emissions at approximately 19% higher total plant costs<sup>43</sup> than a SMR plant without CCS. In this instance, the capture location is highlighted as point 1 in Fig. 13 and the resulting configuration is hereon referred to as SMR with syngas capture. The alternative is to capture a greater quantity of CO<sub>2</sub> from both the combustion and process gas at an overall capture rate of 90%, increasing the total system costs by 79%<sup>43</sup> compared to a standalone SMR plant, which corresponds to point 2 in the figure. This configuration

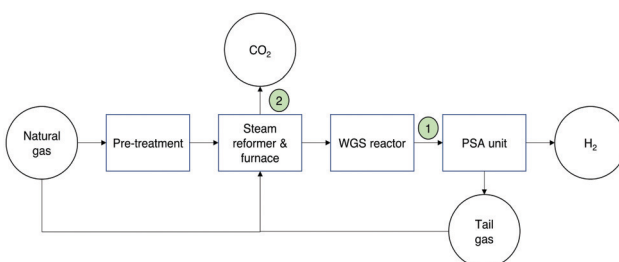


Fig. 13 A schematic overview of the SMR process, indicating the two capture configurations included in this analysis.

is explicitly referred to as the SMR with flue gas capture in the ensuing discussion. The increase in total system costs between the two configurations can be attributed to the dilution of the CO<sub>2</sub> concentration in the flue gas stream. The energetic conversion efficiencies are assumed to be 73% and 70% on a higher heating value (HHV) basis for SMRs with syngas and flue gas capture respectively.<sup>42</sup> The CapEx requirements are assumed to be £320 per kW and £80 per kW for a 1 GW facility of SMRs with syngas capture and flue gas capture on average.<sup>11</sup> All reformer technology costing figures are equivalent to an averaged learning rate induced cost reduction of 8% from current estimates over the time horizon.<sup>102</sup>

**A.2.2 Auto-thermal reforming (ATR).** Fig. 14 shows an ATR process, where some of the natural gas feed is partially combusted with O<sub>2</sub> to produce syngas. Following which, the reforming reactions proceed in the same manner as in SMRs. This process is slightly exothermic with the advantage of offering good response times.<sup>103</sup> The ATR process can be operated at comparatively higher pressures than SMR and produces a syngas mixture with a higher concentration and partial pressure of CO<sub>2</sub>/H<sub>2</sub>. This offers two key benefits: (a) it reduces the total CO<sub>2</sub> capture costs; (b) it reduces the energy requirement for subsequent H<sub>2</sub> compression. In addition, it can achieve higher capture rates economically in comparison to SMRs (up to 95%) due to the higher quantities of CO<sub>2</sub> produced from the O<sub>2</sub> fired process. In contrast to SMRs, the requirement for an Air Separation Unit (ASU) increases its power requirements. A standalone ATR plant with CCS is assumed to operate at an operating pressure of 40 barg, with an efficiency of 78%.<sup>11</sup> The CapEx requirement is estimated as £510 per kW for a 1 GW facility over the time horizon.<sup>11</sup>

**A.2.3 Gas heating reforming (GHR).** GHR or heat exchanger reforming is used to exploit the high temperatures from the gaseous streams downstream of the reforming process to convert more natural gas to H<sub>2</sub> as shown in Fig. 15. GHRs can be integrated with SMRs and ATRs and operated in both series and parallel configurations although there is limited commercial experience in its use. Parallel GHRs are better described than series GHRs at larger scales whereas a series configuration has lower methane slip in addition to higher CO<sub>2</sub>

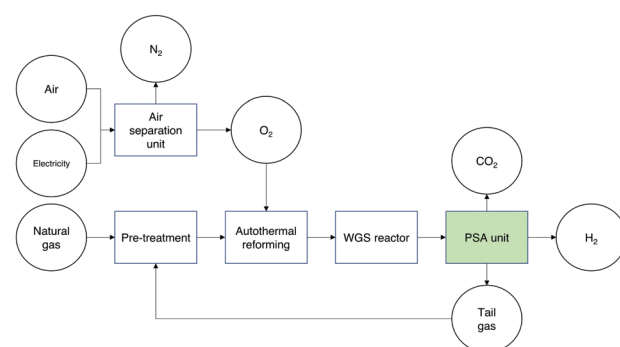


Fig. 14 A schematic overview of the ATR process, indicating the CO<sub>2</sub> capture location in green.



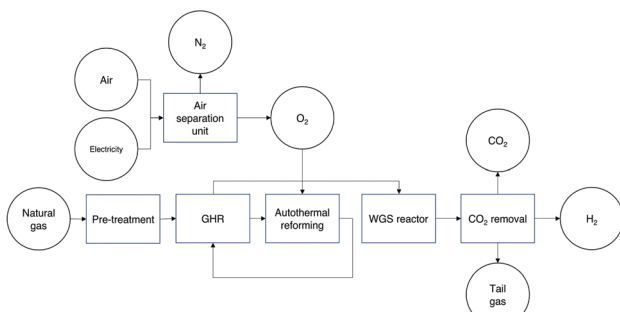


Fig. 15 A schematic overview of the ATR-GHR process.

capture rates.<sup>11,13</sup> For this study, GHRs operated in a parallel configuration with ATRs are considered to operate at 40 barg with a process efficiency of 83%.<sup>11</sup> The total CapEx requirements are defined as £490 per kW on the basis of a 1 GW facility.<sup>11</sup>

**A.2.4 Water electrolysis (WE).** In WE, water molecules are split directly into H<sub>2</sub> and O<sub>2</sub> using an electrolyser. Alkaline electrolysis using potassium hydroxide (KOH) electrolytes is a mature technology, which has been mainly used in WE applications. Technologies such as PEM and most recently, solid oxide electrolysis (SOE) have also been gaining in popularity.<sup>104</sup> WE production systems operate at a variety of scales ranging from a few kW to many MWs. When the WE process is coupled with low-carbon electricity sources, the overall CO<sub>2</sub> footprint is significantly reduced.<sup>105</sup>

In PEM electrolysis, typical output pressures are within 2–4 MPa. All of the electrolyser systems are capable of producing H<sub>2</sub> at purities in excess of 99.95%. Both alkaline and PEM systems have high response rates, allowing for a rapid dispatch of H<sub>2</sub> when necessary. This modelling framework only considers the use of PEM-based electrolyzers for the supply of H<sub>2</sub>. It is assumed that the required power is imported from the existing electricity grid. The model formulation assumes an output pressure of 20 barg with a process efficiency of 72%.<sup>45</sup> There is considerable scope for improvements in the process economics through economies of scale effects as current deployment has largely been limited to niche markets.<sup>106</sup> Secondly, cost reduction potential from technology learning has been estimated to be as high as 31% in Schoots *et al.*<sup>102</sup> A CapEx value of £880 per kW is assumed for the WE process on the basis of 100 MW units.<sup>11,46</sup> The estimate used in this model formulation is equivalent to an averaged learning rate and scale induced cost reduction of 25% from current estimates.

**A.2.5 Biomass gasification (BG).** BG with CCS may have a significant role in the low-carbon H<sub>2</sub> production mix due to its ability to produce H<sub>2</sub> whilst delivering negative emissions.<sup>107</sup> The thermal efficiency of BG is significantly lower than that of fossil fuel based gasification.<sup>107</sup> There are concerns arising from the scarcity of biomass resources and the competition for limited resources in other sectors. BG with CCS is described in the model formulation with explicit definitions of its

dependencies on the electricity/gas infrastructure. The overall process efficiency is assumed to be 40%<sup>49,108</sup> with a H<sub>2</sub> output pressure of 20 barg and an overall CapEx requirement of £1100 per kW on the basis of 200 MW units.<sup>11,47</sup> The net negative emissions contribution at the point of generation is estimated as 0.42 kg CO<sub>2</sub> per kW h.<sup>48</sup>

### A.3 Transportation technologies

**A.3.1 H<sub>2</sub> transport.** H<sub>2</sub> can be transported using distribution technologies such as pipelines, compressed tube trailers, trucks, ships, *etc.* It is envisaged that pipelines will be utilised as the large scale of heating demand renders the aforementioned alternatives unfavourable.<sup>109</sup> In GB, the IMRP, which converts low pressure distribution pipelines to polyethylene pipes, is scheduled to be completed in the early 2030s. Polyethylene pipes are more porous to H<sub>2</sub> than natural gas, although this leakage is expected to be relatively small (0.001%) when compared to the total transported volume.<sup>50</sup>

Pipelines provide H<sub>2</sub> storage opportunities through the linepack capacity of the network, which is less than a quarter of natural gas but it can be used to tackle daily demand variations.<sup>50,110</sup> H<sub>2</sub> transmission pipelines are typically constructed with low-carbon steel with an epoxy coating to prevent any metallic corrosion.<sup>67</sup> At present, there are at least 1600 km of high pressure H<sub>2</sub> pipelines in operation within the EU alone.<sup>111</sup> The costs of constructing a new pipeline depends on many factors – pipeline diameter, the terrain, routing of pipelines, entrenchment, *etc.* On average, the construction costs are assumed to be 20% higher than natural gas.<sup>112</sup> Only transmission pipelines are described in this model formulation due to the availability of existing infrastructure to support low pressure distribution of H<sub>2</sub>. H<sub>2</sub> transmission pipelines of a variety of sizes: 18, 24, 36, 48 inches are described in the formulation.

**A.3.2 CO<sub>2</sub> transport.** Similarly to H<sub>2</sub>, pipelines are the most viable and commonly used method to transport CO<sub>2</sub>.<sup>113</sup> Gaseous CO<sub>2</sub> is typically compressed to pressures above 8 MPa in order to increase its density and reduce transportation costs. In this state, dense phase CO<sub>2</sub> behaves similarly to a compressible liquid with a density of approximately 900 kg m<sup>-3</sup>.<sup>114</sup> In the US alone, at least 2500 km of pipelines are used to transport more than 40 MtCO<sub>2</sub> per year from natural and anthropogenic sources to sites where CO<sub>2</sub> is used for Enhanced Oil Recovery (EOR).<sup>115</sup>

The costs of CO<sub>2</sub> transportation through pipelines depend mainly on the distance and quantity of CO<sub>2</sub> transported. Offshore transportation is considerably more expensive than onshore transport due to the additional infrastructure requirements. In addition to region-specific factors, total costs are greater if there are intermediary compressor stations along the pipeline.<sup>116</sup> Marine transportation of CO<sub>2</sub> via ships is not considered in this study due to the relative proximity of storage sites from the capture sources.

**A.4 Storage technologies.** Geological structures are capable of storing large quantities of gaseous H<sub>2</sub> for long periods of time.<sup>117</sup> Although these structures present many benefits such



as greater working volumes and an ability to achieve higher pressures, they are limited by the need for the presence of a certain type of geology at the storage location. Depleted oil and gas fields, saline aquifers and salt caverns may be used for the storage of H<sub>2</sub>, although there is limited operational experience in the use of the former two.<sup>9</sup> Salt caverns represent the most economical and reliable option for storing H<sub>2</sub> at large scale at present. The costs of constructing a salt cavern depend on many factors – site preparation, working gas capacity, cushion gas requirements, maintenance costs, *etc.* Key locations with development potential for salt caverns were identified in GB by the British Geological Survey (BGS).<sup>83</sup> It is likely that significant expansions in salt cavern capacity will be required for H<sub>2</sub> storage compared to a natural gas based system, due to the limited commercial experience with storage of H<sub>2</sub> *via* alternative technologies.

The model formulation assumes maximum injectivity and deliverability rates of 100 MW and 200 MW per cavern respectively, given volume/pressure constraints.<sup>13</sup> There is uncertainty associated with these figures and they may not be representative of the geological characteristics in all of the storage sites within GB. However, these figures should be realisable as conservative estimates. The H21 North of England study revised their cavern cost estimates from £338 per MW h to £226 per MW h in their recent report.<sup>13</sup> Energy Technologies Institute (ETI) storage appraisals indicate higher costs although there is potential to reduce total costs through sharing the above ground facilities.<sup>53</sup> Additionally, ETI report that total costs of offshore caverns are 75% more expensive than onshore caverns when three caverns are used. However, this is likely to be a pessimistic estimate when considering a greater number of caverns per overground facility as the costs of water and brine pipelines are likely to increase onshore costs relative to offshore costs. The nominal cost for a cavern in this model formulation is assumed to be £500 per MW h with offshore caverns costing approximately 30% greater than the onshore caverns. The relative impact of these assumptions on total annualised system costs is studied in Section 6.3. All caverns are assumed to be sized at 300 000 m<sup>3</sup> and the working capacity is computed based on the operational pressure ranges. A series of geological deposits with formation pressures,  $P^{\max}$  of 105 and 270 bar are distributed across GB. The minimum cavern operating pressure,  $P^{\min}$  is calculated as  $0.3P^{\max}$ .<sup>9</sup> H<sub>2</sub> volumetric energy density under these conditions is used to compute the maximum working capacity per cavern. Consequently, caverns with  $P^{\max}$  of 270 and 105 bar<sup>11</sup> are assumed to have maximum working capacities of 144 and 64 GW h respectively.

The availability of CO<sub>2</sub> storage is central to any H<sub>2</sub> network prospectively considering a reforming-based pathway. When injected, dense phase CO<sub>2</sub> compresses and fills the pore space by displacing the fluids within the pore volume. In depleted oil and gas reservoirs, most of the surface equipment can be reutilised to reduce the total costs associated with storage. The total costs of sequestering a given quantity of CO<sub>2</sub> depends on many factors such as the number of injection wells, well length, site development expenses, *etc.* The total injection rate into a

storage site is determined using the number of injection wells in a site combined with the injectivity per well, which is estimated on average to be approximately 1.5 Mt of CO<sub>2</sub> per year.<sup>56</sup> There are uncertainties as to the maximum achievable injection rates in a given storage basin due to the uncertainties surrounding specific sub-surface interactions. There is considerable scope for improvements in the representation of region-specific geological considerations both in the case of H<sub>2</sub> and CO<sub>2</sub> as in d'Amore *et al.*<sup>118</sup> This may require simplified representations of more detailed dynamic models that are capable of defining parameters such as injection rates based on previously injected volumes.

## Acknowledgements

The authors would like to greatly acknowledge the PhD funding and support received from the ERA-NET ACT project, ELEGANCY. ACT ELEGANCY, Project No. 271498, has received funding from DETEC (CH), BMWi (DE), RVO (NL), Gassnova (NO), BEIS (UK), Gassco, Equinor and Total, and is cofunded by the European Commission under the Horizon 2020 programme, ACT Grant Agreement No. 691712. We are also thankful to Ronny Pini (Imperial College London) and Maria Yliruka (Imperial College London) for helpful discussions and input. Additionally, we would like to thank the four anonymous reviewers for their critical feedback and suggestions.

## Notes and references

- 1 Committee on Climate Change, *Net Zero – Technical report*, May, 2019.
- 2 H. Troup, *Renewable Energy Focus*, 2016, **17**, 178–179.
- 3 European Commission, *An EU Strategy on Heating and Cooling*, European commission technical report, 2016.
- 4 R. Gross and R. Hanna, *Nat. Energy*, 2019, **4**, 358–364.
- 5 Department of Business Energy and Industrial Strategy (BEIS), *Clean Growth – Transforming Heating – Overview of Current Evidence*, 2018.
- 6 Instituto Nacional de Estadística y Geografía, Canada Natural Resources, SENER, U.S. Energy Information Administration and Estados Unidos Mexicanos, *Underground natural gas storage*, 2017.
- 7 U.S. Energy Information Administration, *Underground Natural Gas Working Storage Capacity – U.S. Energy Information Administration*, 2019, [https://www.eia.gov/natural\\_gas/storagecapacity/](https://www.eia.gov/natural_gas/storagecapacity/).
- 8 R. G. Egging and S. A. Gabriel, *Energy Policy*, 2006, **34**, 2762–2778.
- 9 O. Kruck, R. Prelicz and T. Rudolph, *Assessment of the potential, the actors and relevant business cases for large scale and seasonal storage of renewable electricity by hydrogen under-ground storage in Europe*, June, 2014.
- 10 EU GeoCapacity, *Assessing European Capacity for Geological Storage of Carbon Dioxide*, Geus technical report, 2009.



11 I. Walker, B. Madden and T. Foaad, *Hydrogen supply chain evidence base*, Department for business, energy and industrial strategy technical report, 2018.

12 Department for Business Energy & Industrial Strategy, *Greenhouse gas reporting: conversion factors*, 2018, <https://www.gov.uk/government/publications/>.

13 Northern Gas Networks & Equinor & Cadent, *H21 North of England Report*, 2018.

14 European Environment Agency, *Electricity generation – emission intensity*, 2018, <https://www.eea.europa.eu/data-and-maps/daviz/co2-emission-intensity-5>.

15 International Energy Agency, *The Future of Hydrogen*, June, 2019.

16 S. A. van den Heever and I. E. Grossmann, *Comput. Chem. Eng.*, 2003, **27**, 1813–1839.

17 A. Almansoori and N. Shah, *Chem. Eng. Res. Des.*, 2006, **84**, 423–438.

18 A. Almansoori and N. Shah, *Int. J. Hydrogen Energy*, 2009, **34**, 7883–7897.

19 A. Almansoori and N. Shah, *Int. J. Hydrogen Energy*, 2012, **37**, 3965–3977.

20 S. De-León Almaraz, C. Azzaro-Pantel, L. Montastruc and S. Domenech, *Int. J. Hydrogen Energy*, 2014, **39**, 11831–11845.

21 S. De-León Almaraz, C. Azzaro-Pantel, L. Montastruc, L. Pibouleau and O. B. Senties, *Int. J. Hydrogen Energy*, 2013, **38**, 14121–14145.

22 J. Kim, Y. Lee and I. Moon, *Int. J. Hydrogen Energy*, 2008, **33**, 4715–4729.

23 G. Guillén-Gosálbez, F. D. Mele and I. E. Grossmann, *AIChE J.*, 2009, **56**, 650–667.

24 N. Sabio, A. Kostin, G. Guillén-Gosálbez and L. Jiménez, *Int. J. Hydrogen Energy*, 2012, **37**, 5385–5405.

25 N. Johnson and J. Ogden, *Int. J. Hydrogen Energy*, 2012, **37**, 5421–5433.

26 N. V. S. N. Murthy Konda, N. Shah and N. P. Brandon, *Int. J. Hydrogen Energy*, 2011, **36**, 4619–4635.

27 S. Samsatli and N. J. Samsatli, *Appl. Energy*, 2017, **220**, 893–920.

28 S. Samsatli, I. Staffell and N. J. Samsatli, *Int. J. Hydrogen Energy*, 2016, **41**, 447–475.

29 J.-H. Han, J.-H. Ryu and I.-B. Lee, *Int. J. Hydrogen Energy*, 2012, **37**, 5328–5346.

30 Z. Li, D. Gao, L. Chang, P. Liu and E. N. Pistikopoulos, *Int. J. Hydrogen Energy*, 2008, **33**, 5275–5286.

31 P. Nunes, F. Oliveira, S. Hamacher and A. Almansoori, *Int. J. Hydrogen Energy*, 2015, **40**, 16408–16418.

32 A. Almansoori and A. Betancourt-Torcat, *Energy*, 2016, **111**, 414–429.

33 M. Moreno-Benito, P. Agnolucci and L. G. Papageorgiou, *Comput. Chem. Eng.*, 2017, **102**, 110–127.

34 A. C. Weber and L. G. Papageorgiou, *Chem. Eng. Res. Des.*, 2018, **131**, 266–278.

35 S. Samsatli and N. J. Samsatli, *Appl. Energy*, 2019, **233–234**, 854–893.

36 N. Johnson and C. Yang, *Optimal Design of a Fossil Fuel-Based Hydrogen Infrastructure with Carbon Capture and Sequestration: Case Study in Ohio*, National hydrogen association technical report, 2005.

37 S. De-León Almaraz, C. Azzaro-Pantel, L. Montastruc and M. Boix, *Chem. Eng. Res. Des.*, 2015, **104**, 11–31.

38 Department of Business Energy and Industrial Strategy (BEIS), *Sub-national gas consumption data – GOV.UK*, <https://www.gov.uk/government/collections/sub-national-gas-consumption-data>.

39 J. Rosenow, P. Guertler, S. Sorrell and N. Eyre, *Energy Policy*, 2018, **121**, 542–552.

40 Office for National Statistics, *Overview of the UK population*, 2018, <https://www.ons.gov.uk/peoplepopulationandcommunity/populationandmigration/populationestimates/articles/overviewoftheukpopulation/november2018>.

41 R. Sansom, *Decarbonising low grade heat for low carbon future*, October, 2014.

42 IEAGHG, *Techno - Economic Evaluation of SMR Based Standalone (Merchant) Hydrogen Plant with CCS*, February, 2017.

43 G. Collodi, G. Azzaro, N. Ferrari and S. Santos, *Energy Procedia*, 2017, **114**, 2690–2712.

44 J. Meerman, E. Hamborg, T. van Keulen, A. Ramírez, W. Turkenburg and A. Faaij, *Int. J. Greenhouse Gas Control*, 2012, **9**, 160–171.

45 D. Scamman and M. Newborough, *Int. J. Hydrogen Energy*, 2016, **41**, 10080–10089.

46 O. Schmidt, A. Gambhir, I. Staffell, A. Hawkes, J. Nelson and S. Few, *Int. J. Hydrogen Energy*, 2017, **42**, 30470–30492.

47 Ecofys, *Bioenergy Heat Pathways to 2050 – Rapid Evidence Assessment*, 2018.

48 National Renewable Energy Laboratory, *H2A: Hydrogen Analysis Production Case Studies*, 2015, <https://www.nrel.gov/hydrogen/h2a-production-case-studies.html>.

49 Energy Research Partnership, *Potential Role of Hydrogen in the UK Energy System*, October, 2016.

50 D. Haeseldonckx and W. D'haeseleer, *Int. J. Hydrogen Energy*, 2007, **32**, 1381–1386.

51 Zero Emissions Platform, *The Costs of CO<sub>2</sub> Capture, Transport and Storage*, 2011.

52 Gas Storage Europe, *GIE – Gas Infrastructure Europe – Maps & Data*, [http://www.gie.eu/maps\\_data/storage.asp](http://www.gie.eu/maps_data/storage.asp).

53 Energy Technologies Institute, *The role of hydrogen storage in a clean responsive power system*, 2015.

54 Northern Gas Networks, *The H21 City Gate Project*, 2016.

55 National Institute of Standards and Technology, *Thermophysical Properties of Fluid Systems*, <https://webbook.nist.gov/chemistry/fluid/>.

56 S. A. Mathias, J. G. Gluyas, W. H. Goldthorpe and E. J. Mackay, *Environ. Sci. Technol.*, 2015, **49**, 13510–13518.

57 C. C. Pantelides, *Proceedings on the second conference on foundations of computer aided operations*, 1994, pp. 253–274.

58 X. Zhang and R. Sargent, *Comput. Chem. Eng.*, 1996, **20**, 897–904.

59 G. Schilling and C. Pantelides, *Comput. Chem. Eng.*, 1996, **20**, S1221–S1226.

60 G. Schilling and C. Pantelides, *Comput. Chem. Eng.*, 1999, **23**, 635–655.



61 A. Dimitriadis, N. Shah and C. Pantelides, *Comput. Chem. Eng.*, 1997, **21**, S1061–S1066.

62 P. Castro, A. P. F. D. Barbosa-Pó and H. Matos, *Ind. Eng. Chem. Res.*, 2001, **40**, 2059–2068.

63 P. M. Castro, A. P. Barbosa-Pó and H. A. Matos, *Ind. Eng. Chem. Res.*, 2003, **42**, 3346–3360.

64 P. Castro, H. Matos and A. Barbosa-Póvoa, *Comput. Chem. Eng.*, 2002, **26**, 671–686.

65 S. Samsatli, N. J. Samsatli and N. Shah, *Appl. Energy*, 2015, **147**, 131–160.

66 M. Dorrington, M. Lewitt, I. Summerfield, P. Robson and J. Howes, *Desk study on the development of a hydrogen-fired appliance supply chain*, July, 2016.

67 P. E. Dodds, I. Staffell, A. D. Hawkes, F. Li, P. Grunewald, W. McDowall and P. Ekins, *Int. J. Hydrogen Energy*, 2015, **40**, 2065–2083.

68 J. Keirstead and N. Shah, *Urban energy systems: an integrated approach*, Routledge, 2013, p. 312.

69 A. A. Saltelli, *Global sensitivity analysis: the primer*, John Wiley, 2008, p. 292.

70 S. Pye, N. Sabio and N. Strachan, *Energy Policy*, 2015, **87**, 673–684.

71 GAMS, *General Algebraic Modeling System – Download*, <https://www.gams.com/download/>.

72 Python.org, *Python 2.7.0 Release*, <https://www.python.org/download/releases/2.7/>.

73 QGIS, *QGIS – The Leading Open Source Desktop GIS*, 2017, <https://www.qgis.org/en/site/about/index.html>.

74 G. Strbac, D. Pudjianto, R. Sansom, P. Djapic, H. Ameli, N. Shah, N. Brandon and A. Hawkes, *Analysis of Alternative UK Heat Decarbonisation Pathways*, August, 2018.

75 Element Energy & E4tech, *Cost analysis of future heat infrastructure options*, 2018.

76 G. Fiorese and G. Guariso, *Environ. Modell. Softw.*, 2010, **25**, 702–711.

77 F. van der Hilst, V. Dornburg, J. Sanders, B. Elbersen, A. Graves, W. Turkenburg, H. Elbersen, J. van Dam and A. Faaij, *Agric. Syst.*, 2010, **103**, 403–417.

78 P. Feron, A. Cousins, K. Jiang, R. Zhai, S. Shwe Hla, R. Thiruvenkatachari and K. Burnard, *Int. J. Greenhouse Gas Control*, 2019, 188–202.

79 D. Zhang, M. Bui, M. Fajard, P. Patrizio, F. Kraxner and N. M. Dowell, *Sustainable Energy Fuels*, 2019, **4**, 226–253.

80 Department for Business Energy & Industrial Strategy, *Digest of UK Energy Statistics (DUKES): natural gas*, <https://www.gov.uk/government/statistics/>.

81 C. F. Heuberger, I. Staffell, N. Shah and N. M. Dowell, *Comput. Chem. Eng.*, 2017, **107**, 247–256.

82 P. Taylor, O. Lavagne D'ortigue, N. Trudeau and M. Francoeur, *Energy Efficiency Indicators for Public Electricity Production from Fossil Fuels*, International energy agency technical report, 2008.

83 D. Parkes, D. J. Evans, P. Williamson and J. D. Williams, *J. Energy Storage*, 2018, **18**, 50–61.

84 M. Bentham, T. Mallows, J. Lowndes and A. Green, *Energy Procedia*, 2014, pp. 5103–5113.

85 D. M. Reiner, *Nat. Energy*, 2016, **1**, 1–7.

86 P. E. Dodds and S. Demoullin, *Int. J. Hydrogen Energy*, 2013, **38**, 7189–7200.

87 S. Arapostathis, P. J. Pearson and T. J. Foxon, *Environ. Innov. Soc. Trans.*, 2014, **11**, 87–102.

88 D. Newbery, M. Pollitt, D. Reiner and S. Taylor, *Cambridge Working Papers in Economics*, 2019, **1969**, 6.

89 D. Makovsek and D. Veryard, *The Regulatory Asset Base and Project Finance Models*, International transport forum technical report, 2016.

90 Her Majesty's Treasury, *The Green Book – Central Government Guidance on Appraisal and Evaluation*, 2018.

91 Department for Business Energy & Industrial Strategy, *2017 Fossil Fuel Price Assumptions*, 2017.

92 Committee on Climate Change, *Biomass in a low-carbon economy*, November, 2018.

93 EDF Energy, *What makes up your energy bill?*, 2019, <https://www.edfenergy.com/for-home/help-support/what-makes-up-your-bill>.

94 Statista, *Forecasted gas prices in the United Kingdom from 2017 to 2023 (in pence per therm\*)*, 2019, <https://www.statista.com/statistics/374970/united-kingdom-uk-gas-price-forecast/>.

95 Á. Morales-García, A. Fernández-Fernández, F. Viñes and F. Illas, *J. Mater. Chem. A*, 2018, **6**, 3381–3385.

96 T. Takata, J. Jiang, Y. Sakata, M. Nakabayashi, N. Shibata, V. Nandal, K. Seki, T. Hisatomi and K. Domen, *Nature*, 2020, **581**, 411–414.

97 Y. X. Chen, A. Lavacchi, H. A. Miller, M. Bevilacqua, J. Filippi, M. Innocenti, A. Marchionni, W. Oberhauser, L. Wang and F. Vizza, *Nat. Commun.*, 2014, **5**, 1–6.

98 Process Systems Enterprise Ltd, *gPROMS Process Modelling Software*, 2017, <https://www.psenterprise.com/products/gproms>.

99 M. V. Twigg, *Catalyst handbook*, The CRC Handbook of Chemistry and Physics, 1989.

100 National Research Council (US) Committee on Alternatives and Strategies for Future Hydrogen Production and Use, National Academy of Engineering and National Academy of Sciences (U.S.), *The hydrogen economy: opportunities, costs, barriers, and R & D needs*, National Academies Press, 2004, p. 239.

101 K. Zeng and D. Zhang, *Prog. Energy Combust. Sci.*, 2010, **36**, 307–326.

102 K. Schoots, F. Ferioli, G. Kramer and B. van der Zwaan, *Int. J. Hydrogen Energy*, 2008, **33**, 2630–2645.

103 J. Holladay, J. Hu, D. King and Y. Wang, *Catal. Today*, 2009, **139**, 244–260.

104 S. Grigoriev, V. Porembsky and V. Fateev, *Int. J. Hydrogen Energy*, 2006, **31**, 171–175.

105 C. Acar and I. Dincer, *Causes, Impacts and Solutions to Global Warming*, Springer New York, New York, NY, 2013, pp. 493–514.

106 E4tech Sàrl & Element Energy Ltd, *Development of Water Electrolysis in the European Union – Fuel cells and Hydrogen Joint Undertaking*, 2014.

107 O. Yamada, *Thin Solid Films*, 2006, **509**, 207–211.



108 D. Hart, J. Howes, F. Lehner, P. E. Dodds, N. Hughes, B. Fais, N. Sabio and M. Crowther, *Scenarios for deployment of hydrogen in contributing to meeting carbon budgets and the 2050 target Final Report Title Scenarios for deployment of hydrogen in contributing to meeting carbon budgets and the 2050 target*, 2015.

109 M. Pudukudy, Z. Yaakob, M. Mohammad, B. Narayanan and K. Sopian, *Renewable Sustainable Energy Rev.*, 2014, **30**, 743–757.

110 H2FC Supergenhub, *The role of hydrogen and fuel cells in delivering energy security for the UK*, March, 2017.

111 J. Perrin, R. Steinberger-Wilckens and S. C. Trümper, *Deliverable 2.1 and 2.1a – “European Hydrogen Infrastructure Atlas” and “Industrial Excess Hydrogen Analysis”*, 2007.

112 B. van der Zwaan, K. Schoots, R. Rivera-Tinoco and G. Verbong, *Appl. Energy*, 2011, **88**, 3821–3831.

113 R. Svensson, M. Odenberger, F. Johnsson and L. Strömberg, *Energy Convers. Manage.*, 2004, **45**, 2343–2353.

114 H. A. Haugen, N. Eldrup, C. Bernstone, S. Liljemark, H. Pettersson, M. Noer, J. Holland, P. A. Nilsson, G. Hegerland and J. O. Pande, *Energy Procedia*, 2009, **1**, 1665–1672.

115 P. N. Seevam, J. M. Race, M. J. Downie and P. Hopkins, *2008 7th International Pipeline Conference*, 2008, vol. 1, pp. 39–51.

116 Intergovernmental Panel on Climate Change, *Carbon dioxide capture and storage*, October, 2009.

117 A. Ozarslan, *Int. J. Hydrogen Energy*, 2012, **37**, 14265–14277.

118 F. D'Amore, N. Sunny, D. Iruretagoyena, F. Bezzo and N. Shah, *Comput. Chem. Eng.*, 2019, **129**, 106521.

